JAERI-M
84-041

ANALYSIS OF TRAC-PD2 PREDICTION FOR THE CYLINDRICAL CORE TEST FACILITY EVALUATION-MODEL TEST C1-19 (RUN 38)

March 1984

Hajime AKIMOTO

日本原子力研究所
Japan Atomic Energy Research Institute

JAERI-Mレポートは，日本原子力研究所が不定期に公刊している研究報告書です。
入手の問合わせは，日本原子力研究所技術情報部情報資料課（〒319-11茨城県那珂郡東海村）あて，お申しこしください。なお，このほかに財団法人原子力弘済会資料センター（〒319-11 茨城県那珂郡東海村日本原子力研究所内）で複写による実費頒布をおこなっております。

JAERI-M reports are issued irregularly.
Inquiries about availability of the reports should be addressed to Information Section, Division of Technical Information, Japan Atomic Energy Research Institute, Tokai-mura, Naka-gun, Ibaraki-ken 319-11, Japan.

編集兼発行　日本原子力研究所
印　　刷　いばらき印刷㈱

JAERI-M 84-041

ANALYSIS OF TRAC-PD2 PREDICTION FOR THE CYLINDRICAL CORE TEST FACILITY EVALUATION-MODEL TEST C1-19 (RUN 38)

Hajime AKIMOTO

Department of Nuclear Safety Research,
Tokai Research Establishment, JAERI

(Received January 31, 1984)

The results of TRAC-PD2 post-test analysis for the CCTF Evaluation Model Test (Run 38) were analyzed to assess the capability of the TRAC code for the prediction of the thermal-hydraulic behavior during a loss-of-coolant accident of a pressurized water reactor. Through the comparisons with CCTF test results, it was found that the accuracy of the TRAC prediction of the turnaround behavior of heater rods was decreased due to the overestimation of the downcomer-to-core U-tube-type oscillation in the early period of the reflood (before 200 s in the CCTF test). For the later period of the reflood (after 200 s in the CCTF test), TRAC overestimated the core water accumulation rate and underestimated the carry-over from the upper plenum to the primary loops, the loop mass flow rate; and the heat transfer from the secondary side to the primary side of the steam generator. However, these errors cancelled each other in the TRAC calculation and allowed excellent agreement of the core inlet mass flow rate and the quench time of heater rods in the later period of the reflood. As a summary of data comparisons, a review was recommended for the hydraulic model in the vessel to clarify why TRAC overestimates the downcomer-to-core U-tube-type oscillation in the early period of the reflood, the hydraulic model in the vessel to clarify why TRAC overestimates the water accumulation rate in the core and underestimates the water carry-over to the primary loops. A separate calculation for the loop thermal-hydraulic behavior in the CCTF test was also recommended to improve the loop flow resistance model and the steam generator heat transfer model in the TRAC code.

The work was performed under contract with the Atomic Energy Bureau of Science and Technology Agency of Japan.

The predicted flow behavior in the pressure vessel was surveyed on a time averaged basis. TRAC results showed asymmetric velocity profiles in the core, the downcomer and the upper plenum. TRAC results suggested that the multidimensional effect was not negligible in the CCTF test. However, the reliability of the TRAC prediction is uncertain at present because there was no experimental basis for the multidimensional flow in the CCTF test. A sensitivity study with TRAC is recommended to get more information on the multidimensional flow behavior in the CCTF tests. It is necessary to study more in order to clarify the effect of the multidimensional flow behavior both experimentally and analytically.

Keywords: PWR, LOCA, Reflood, CCTF, Heat Transfer, Two-Phase Flow, TRAC Code, Multidimensional Thermo-Hydrodynamics, Comparative Evaluations

JAERI － M 84 － 041

円筒炉心試験評価モデル試験C1－19（Run 38）に対するTRAC－PD2計算結果の検討

日本原子力研究所東海研究所安全工学部
秋本　肇

（1984年1月31日受理）

加圧水型原子炉の冷却材喪失事故再冠水時の熱水力挙動に関するTRACコード（PD2バージョン）の予測性能評価を目的として，円筒炉心試験評価モデル試験C1－19（Run 38）を例に，TRACコードによる計算結果と試験結果との比較検討を行った。

試験結果との比較から，再冠水初期にみられるダウンカマ炉心間のU字管型振動が過大評価されることにより発熱棒のターンアラウンド温度の予測精度が低められていることがわかった。また再冠水後期では，試験結果と比べて炉心内蓄水速度を過大に評価する一方で，上部プレナムから一次系ループへのキャリーオーバ水量・一次系ループ流量・蒸気発生器での伝熱量を過小に評価していることがわかった。しかし再冠水後期においては，これらの評価誤差は互いに打消しあい，炉心冠水速度や発熱棒のクエンチ時刻の計算結果は試験結果とよく一致している。今後TRACコードによる再冠水熱水力挙動の予測精度を向上するためには，再冠水初期のダウンカマ炉心間のU字管型振動過大評価の原因，並びに，再冠水後期の炉心内蓄水速度の過大評価と上部プレナムからのキャリーオーバ水量の過小評価の原因を究明することが必要である。またTRACコードの一次系ループ流動抵抗モデルと蒸気発生器伝熱モデルを改良するために，円筒炉心試験のループ部熱水力挙動に着目した計算を行うことを推奨する。

TRACコードにより予測された圧力容器内流動について，時間平均値を用いて検討を行った。炉心・ダウンカマ・上部プレナムにおいて，TRACコードは非対称な速度分布を計算し，円筒炉心試験では三次元的な流動が起こることを示唆した。試験結果との比較ができなかったことから，これらの多次元的な流動については計算結果の信頼度を評価できなかった。今後TRAC計算結果の信頼度を確かめるために，感度解析を行う必要があると考える。多次元的な流動の影響を明らかにするために，実験・解析の両面から今後さらに検討をすすめることが必要である。

本報告書は，電源開発促進対策特別会計法に基づき，科学技術庁からの受託によって行った研究の成果である。

Contents

目　　次

List of Tables

List of Figures

1. INTRODUCTION

The Cylindrical Core Test Facility (CCTF) is an experimental test facility designed to provide information on the thermal-hydraulic behavior during the refill and reflood phases of a hypothetical loss-of-coolant accident of a pressurized water reactor (PWR). This facility has a full-height core section with about 2,000 electrically heated rods arranged in a cylindrical array and has four primary loops with reactor component simulations. The system integral effects and the cooling characteristics of the core are being investigated to demonstrate the effectiveness of Emergency Core Cooling System (ECCS), to verify computer codes, and to collect information to improve the thermo-hydraulic models in analysis codes.[1]

The PWR version of the Transient Reactor Analysis Code (TRAC) is being developed at the Los Alamos National Laboratory to provide an advanced best-estimate predictive capability for the analysis of postulated accidents in PWRs.[2] TRAC is being used to provide analysis support to a multinational experimental and analytical research program (known as 2D/3D program) investigating multidimensional thermal-hydraulic behavior during loss-of-coolant accidents in large pressurized water reactors. The TRAC calculations that have been performed at the Los Alamos National Laboratory for CCTF[3,4] can be grouped into two broad categories. One is termed the coarse node calculations. This type of calculation was performed to demonstrate that TRAC-PD2 can account for the overall parametric effects during reflood. Los Alamos investigated the effects of the Emergency Core Coolant (ECC) flow rate and system pressure on the quench behavior of the electrically heated core.[3] The analysis results have demonstrated that TRAC-PD2 can account for these effects qualitatively during reflood. The second type of calculation uses fine noding to demonstrate that TRAC-PD2 can quantitatively predict the detailed thermal-hydraulic behavior.[4] The objective of this report is to discuss the results of the fine-node TRAC calculation and the CCTF test data[5] for Test C1-19 (Run 38); and to assess the TRAC calculation by comparisons to data.

2. TEST FACILITY AND TRAC INPUT

The overall schematic diagram of the CCTF is shown in Fig. 1.[5]

1. INTRODUCTION

The Cylindrical Core Test Facility (CCTF) is an experimental test facility designed to provide information on the thermal-hydraulic behavior during the refill and reflood phases of a hypothetical loss-of-coolant accident of a pressurized water reactor (PWR). This facility has a full-height core section with about 2,000 electrically heated rods arranged in a cylindrical array and has four primary loops with reactor component simulations. The system integral effects and the cooling characteristics of the core are being investigated to demonstrate the effectiveness of Emergency Core Cooling System (ECCS), to verify computer codes, and to collect information to improve the thermo-hydraulic models in analysis codes.[1]

The PWR version of the Transient Reactor Analysis Code (TRAC) is being developed at the Los Alamos National Laboratory to provide an advanced best-estimate predictive capability for the analysis of postulated accidents in PWRs.[2] TRAC is being used to provide analysis support to a multinational experimental and analytical research program (known as 2D/3D program) investigating multidimensional thermal-hydraulic behavior during loss-of-coolant accidents in large pressurized water reactors. The TRAC calculations that have been performed at the Los Alamos National Laboratory for CCTF[3,4] can be grouped into two broad categories. One is termed the coarse node calculations. This type of calculation was performed to demonstrate that TRAC-PD2 can account for the overall parametric effects during reflood. Los Alamos investigated the effects of the Emergency Core Coolant (ECC) flow rate and system pressure on the quench behavior of the electrically heated core.[3] The analysis results have demonstrated that TRAC-PD2 can account for these effects qualitatively during reflood. The second type of calculation uses fine noding to demonstrate that TRAC-PD2 can quantitatively predict the detailed thermal-hydraulic behavior.[4] The objective of this report is to discuss the results of the fine-node TRAC calculation and the CCTF test data[5] for Test C1-19 (Run 38); and to assess the TRAC calculation by comparisons to data.

2. TEST FACILITY AND TRAC INPUT

The overall schematic diagram of the CCTF is shown in Fig. 1.[5]

The CCTF is designed to model a full-height core section and four primary loops of a PWR. The central part of this facility is the pressure vessel which includes a downcomer, lower plenum, core and upper plenum. The facility is equipped with four loops that are composed of three intact loops and a broken loop which simulates cold leg large break. The ECCS in the CCTF consists of an accumulator (Acc) and a low pressure coolant injection (LPCI) system. The ECC water is injected into the primary system through the lower plenum injection nozzle or cold leg injection nozzles.

Figure 2 shows the dimensions of the pressure vessel in the CCTF. The height is the same as that of a full-scale PWR. The radial size is scaled down in proportion to the core scaling factor, 1/21.4. The core consists of 32 8×8 electrically heated rod bundles arranged in a cylindrical configuration. The downcomer is an annulus of 61.5 mm gap. The outside wall of the downcomer (the pressure vessel wall) is constructed of carbon steel cladded with 5 mm stainless steel plate. The vessel wall thickness is 90 mm. The internals of the upper plenum are scaled down by factor of 8/15 from those of the reference reactor.

Figure 3 shows the TRAC noding schematic for the fine-node model.[4] The primary loops are modeled by the combination of PIPE, STGEN, and TEE components in the TRAC-PD2 code. A BREAK component is used to model the containment tank and provides a pressure boundary condition similar to the facility. The boundary conditions of the ECC water injection are specified with FILL components connected to VESSEL and TEE components.

Figure 4 shows the TRAC noding schematic for the vessel of the fine-node model. The CCTF pressure vessel is modeled with 4 radial rings, 4 azimuthal sectors and 16 levels. The fourth ring models the downcomer. The lower plenum ECC injection line is connected to the first level. Each cold leg is connected to the fifteenth level at the fourth ring. The broken loop is connected to the first azimuthal cell. The lower plenum, core and upper plenum are modeled by the inner three rings. The core extends axially from the fourth level to the tenth level.

3. TEST PROCEDURE AND CONDITIONS

The test procedure of the CCTF TEST C1-19 was as follows: After establishing the initial conditions of the test, the lower plenum was

The CCTF is designed to model a full-height core section and four primary loops of a PWR. The central part of this facility is the pressure vessel which includes a downcomer, lower plenum, core and upper plenum. The facility is equipped with four loops that are composed of three intact loops and a broken loop which simulates cold leg large break. The ECCS in the CCTF consists of an accumulator (Acc) and a low pressure coolant injection (LPCI) system. The ECC water is injected into the primary system through the lower plenum injection nozzle or cold leg injection nozzles.

Figure 2 shows the dimensions of the pressure vessel in the CCTF. The height is the same as that of a full-scale PWR. The radial size is scaled down in proportion to the core scaling factor, 1/21.4. The core consists of 32 8×8 electrically heated rod bundles arranged in a cylindrical configuration. The downcomer is an annulus of 61.5 mm gap. The outside wall of the downcomer (the pressure vessel wall) is constructed of carbon steel cladded with 5 mm stainless steel plate. The vessel wall thickness is 90 mm. The internals of the upper plenum are scaled down by factor of 8/15 from those of the reference reactor.

Figure 3 shows the TRAC noding schematic for the fine-node model.[4] The primary loops are modeled by the combination of PIPE, STGEN, and TEE components in the TRAC-PD2 code. A BREAK component is used to model the containment tank and provides a pressure boundary condition similar to the facility. The boundary conditions of the ECC water injection are specified with FILL components connected to VESSEL and TEE components.

Figure 4 shows the TRAC noding schematic for the vessel of the fine-node model. The CCTF pressure vessel is modeled with 4 radial rings, 4 azimuthal sectors and 16 levels. The fourth ring models the downcomer. The lower plenum ECC injection line is connected to the first level. Each cold leg is connected to the fifteenth level at the fourth ring. The broken loop is connected to the first azimuthal cell. The lower plenum, core and upper plenum are modeled by the inner three rings. The core extends axially from the fourth level to the tenth level.

3. TEST PROCEDURE AND CONDITIONS

The test procedure of the CCTF TEST C1-19 was as follows: After establishing the initial conditions of the test, the lower plenum was

filled with saturated water to a level of 0.89 m. Electric power was supplied to the heater rods of the core at 0 s. The ratios of the power supplied to a rod of three radially divided zones to the averaged power were 1.299, 1.092, and 0.841. When the maximum temperature of heater rods reached the specified temperature (1117 K), the accumulator water injection into the lower plenum was initiated at 93 s. The water level in the pressure vessel reached the bottom of the core at 102 s. A decay of the core heating power was started at the time. Heating power was changed by following the decay curve type of (ANS×1.2+Actinide (30 s after scram)). At 107 s, the injection location of the accumulator was changed from the lower plenum to the ECC injection nozzles of the three intact cold legs. At 118.5 s, the water injection mode was transferred from the accumulator mode to the LPCI mode. The pressure in the containment tank was controlled during the test to keep it constant (0.20 MPa).

The test conditions of CCTF test C1-19 (Run 38) are summarized in Table 1. The TRAC calculation was performed in a manner very similar to that of the actual execution of the test. The time dependent boundary conditions were applied to the core power, the pressure in the containment tank, the ECC flow rate and the ECC water temperature. This information was obtained from the measured data.

4. DATA COMPARISONS AND DISCUSSION

4.1 Overall Thermohydraulic Behavior

4.1.1 Core Inlet Mass Flow Rate

Figure 5 shows the predicted core inlet mass flow rate. The TRAC result shows significant oscillations in the flow rate. The amplitude sometimes reaches over 100 kg/s. The reliability of this result cannot be judged by the direct comparison with the data because no direct measurement of the core inlet mass flow rate was obtained in the CCTF experiment.

Based on the mass balance in the vessel, the core inlet mass flow rate m_F is expressed by the summation of the core water accumulation rate m_{CR}, the upper plenum water accumulation rate m_{UP} and the mass flow rate vented from the upper plenum through the four primary loops m_L:

filled with saturated water to a level of 0.89 m. Electric power was supplied to the heater rods of the core at 0 s. The ratios of the power supplied to a rod of three radially divided zones to the averaged power were 1.299, 1.092, and 0.841. When the maximum temperature of heater rods reached the specified temperature (1117 K), the accumulator water injection into the lower plenum was initiated at 93 s. The water level in the pressure vessel reached the bottom of the core at 102 s. A decay of the core heating power was started at the time. Heating power was changed by following the decay curve type of (ANS×1.2+Actinide (30 s after scram)). At 107 s, the injection location of the accumulator was changed from the lower plenum to the ECC injection nozzles of the three intact cold legs. At 118.5 s, the water injection mode was transferred from the accumulator mode to the LPCI mode. The pressure in the containment tank was controlled during the test to keep it constant (0.20 MPa).

The test conditions of CCTF test C1-19 (Run 38) are summarized in Table 1. The TRAC calculation was performed in a manner very similar to that of the actual execution of the test. The time dependent boundary conditions were applied to the core power, the pressure in the containment tank, the ECC flow rate and the ECC water temperature. This information was obtained from the measured data.

4. DATA COMPARISONS AND DISCUSSION

4.1 Overall Thermohydraulic Behavior

4.1.1 Core Inlet Mass Flow Rate

Figure 5 shows the predicted core inlet mass flow rate. The TRAC result shows significant oscillations in the flow rate. The amplitude sometimes reaches over 100 kg/s. The reliability of this result cannot be judged by the direct comparison with the data because no direct measurement of the core inlet mass flow rate was obtained in the CCTF experiment.

Based on the mass balance in the vessel, the core inlet mass flow rate m_F is expressed by the summation of the core water accumulation rate m_{CR}, the upper plenum water accumulation rate m_{UP} and the mass flow rate vented from the upper plenum through the four primary loops m_L:

$$m_F = m_{CR} + m_{UP} + m_L \quad . \tag{1}$$

By the integration of Eq. (1), the total core inlet mass flow M_F is given by

$$M_F = M_{CR} + M_{UP} + M_L \quad , \tag{2}$$

Where M_{CR}, M_{UP}, and M_L show the core liquid mass, the upper plenum liquid mass and the vented mass through the four primary loops, respectively.

Figure 6 shows the comparison of the total core inlet mass flow M_F between the CCTF and the TRAC results. The CCTF results was evaluated by Eq. (2) using the diffential pressures in the core and the upper plenum, and the mass flow through the loops. The TRAC result was calculated by the integration of the predicted core inlet mass flow rate. The TRAC result shows oscillations between 100 and 200 s, which was not seen in the CCTF result. The oscillations in the TRAC results are mainly due to the downcomer-to-core U-tube-type oscillations.[4] Water in the core is forced to flow back into the lower plenum and the downcomer. This results in the underestimation of the total core inlet flow in the TRAC calculation. After 200 s, the oscillations are not so significant and the predicted slope of the total core inlet mass flow, which corresponds to the time-averaged core inlet mass flow rate, shows excellent agreement with the CCTF results.

Figure 7 shows the comparison of each term in Eq. (2). The mean slopes of M_F, M_{CR}, and M_L between 300 and 500 s are summarized in Table 2. Table 2 shows that TRAC overestimates the core water accumulation rate and underestimates the vented mass flow rate through the four primary loops. Because these errors are cancelling, the excellent agreement in the core inlet mass flow rate with the CCTF result is obtained in the TRAC calculation. This fact suggests the need for future improvement of the core hydraulics and also a review of the loop flow model.

4.1.2 Fluid Temperature at the Core Inlet

Figure 8 shows the comparison of the fluid temperature at the core inlet. The TRAC result shows a low fluid temperature at 110 s but then

a quick temperature rise between 110 and 140 s. On the contrary, the CCTF result does not show the quick rise in the fluid temperature. The temperature drops gradually until 200 s and slowly recovers. In the TRAC calculation, the significant downcomer-to-core U-tube-type oscillations were predicted and water, which was heated to saturation temperature in the core, flowed back into the lower plenum. It can be considered that the flow reversal from the core to the lower plenum resulted in the quick rise of the core inlet fluid temperature in the TRAC calculation. The discrepancy shown above also suggests the overestimation of the oscillations in the TRAC calculation.

4.1.3 Core Inlet Pressure

Figure 9 shows the comparison of the core inlet pressure. The agreement between the TRAC and CCTF results is rather good. The TRAC result shows excellent agreement with the CCTF result before 120 s. But at 120 s, the TRAC result shows a stepwise pressure decrease that is not evident in the CCTF result. TRAC predicts lower core inlet pressure than the CCTF result between 120 and 400 s.

The core inlet pressure P_{CR} is expressed by the equation:

$$P_{CR} = P_{CN} + \Delta P_{BCL} + \Delta P_{D} \quad , \tag{3}$$

where P_{CN} indicates the containment pressure, ΔP_{BCL} indicates the pressure drop through the broken cold leg and ΔP_{D} indicates the downcomer water head. To make clear the origin of the discrepancy in the core inlet pressure, each term of Eq. (3) is compared in Fig. 10. A stepwise decrease in ΔP_{D} is predicted at 120 s. This means that the downcomer fluid is spilled over through broken cold leg and lost from the pressure vessel because of the overestimation of the downcomer-to-core U-tube-type oscillations. The TRAC result shows excellent agreement with the CCTF result for ΔP_{D} after 200 s. The predicted ΔP_{BCL} is smaller than the experimental value until 400 s. The discrepancy in P_{CR} evaluation is caused mainly by the error in the ΔP_{BCL} estimation between 200 and 400 s.

Through the comparisons of ΔP_{CN}, ΔP_{BCL}, and ΔP_{D}, it is recommended to study the downcomer-to-core U-tube-type oscillations and to review the calculation model of ΔP_{BCL}.

4.2 Loop Thermohydraulic Behavior

4.2.1 Mass Flow Rate and Differential Pressure

Figure 11 shows the predicted mass flow rate through each primary loop and Fig. 12 shows the integrated results of the mass flow rate. The predicted mass flow rate through the three intact loops are almost identical and no parallel channel oscillation is predicted. The mass flow rate through the broken loop is about 50 per cent higher than that of the intact loop. These predicted tendencies are consistent with the observed results in the CCTF tests.

Figure 13 shows the comparison of the mass flow rate and the total pressure drop through an intact loop. TRAC underestimates the mass flow rate and overestimates the total pressure drop. This indicates the overestimation of the overall flow resistance of the intact loop in the TRAC calculation.

Figure 14 shows the comparisons of the component-by-component differential pressure for the intact loop. The time averaged values of these differential pressures are summarized in Table 3. The TRAC result shows the overestimation for the differential pressures (D/Ps) through the steam generator and the cold leg, while it shows the underestimation for the DP through the hot leg. The predicted DP through the pump orifice and the loop seal show good agreement with the CCTF results. The predicted mass flow rate through the intact loop is about 20 per cent lower than the measured rate, while the total differential pressure is about 25 per cent higher than the measured ΔP as shown in Table 3. It can be considered that the loop flow resistance coefficient in the TRAC calculation is 65 per cent higher than that in the CCTF.

The accurate estimation of the mass flow rate through the primary loop is essential to predict the correct core inlet mass flow rate as can be seen in Table 2. Therefore, the review of the loop flow resistance is recommended for future improvement.

4.2.2 Heat Transfer at the Steam Generator

Figure 15 shows the comparison of the fluid temperature at the inlet and outlet plenums of the steam generator. The TRAC results show the higher inlet and outlet fluid temperature than the CCTF results.

Figure 16 shows the comparison of the fluid temperature in the

secondary side of the steam generator. In the TRAC calculation, the secondary side temperature is nearly constant regardless of time at each elevation, while the CCTF result show the significant temperature decrease during the test. Figure 17 shows the comparison of the total energy transferred from the secondary side to the primary side of the steam generator. The transferred energy is underestimated in the TRAC calculation.

Figure 18 shows the predicted void fraction in the intact hot leg. The void fraction is unity for almost all periods. This result shows that almost no water carry-over from the upper plenum to the intact loop in the TRAC calculation. On the contrary, annular or dispersed flow was observed at the hot leg of the CCTF during the test. It seems that the underestimation of the total energy transferred from the secondary side to the primary side of the steam generator is caused mainly by the error in the estimation of the carry-over to the hot leg.

The separate calculation of the steam generator is recommended to confirm the heat transfer model of the TRAC code with the known inlet thermohydraulic conditions.

4.3 Core Thermal Behavior

Figure 19 shows the comparison of the rod surface temperature at the core midplane of the medium power rod in each power region. The power ratios of each power region to the core average linear power are 1.299 (high power region), 1.092 (medium power region), and 0.841 (low power region), as shown in Table 1. The reflood of the core was initiated at 102 s in the test. Before 102 s, the calculated rod temperatures show good agreement with the CCTF results at all power regions. This indicates that the material properties included in the code are correct.

Figures 20 through 22 show the comparisons of the turnaround time, temperature and the quench time, respectively.

Figure 20 shows the comparison of the turnaround time between the TRAC and CCTF results. The turnaround time shows the time after the reflood initiation (t = 102 s) to the time when the maximum temperature is realized. In the high power region, the TRAC calculation over-estimates the turnaround time. In the medium power region, the TRAC calculation shows rather good agreement with the CCTF results, even

though there is a slight underestimation at the upper part of the core. In the low power region, the TRAC calculation underestimates the turnaround time. The turnaround time varies from 0 to 100 s. It is this period that the oscillations are calculated by the TRAC code due to the downcomer-to-core U-tube-type oscillation, which was not so noticeable in the CCTF test. Figure 21 shows the comparison of the turnaround temperature. In the high power region, the TRAC results show the excellent agreement with the CCTF results. While the turnaround temperatures are underestimated by 50K in the medium and low power regions. As shown in Fig. 5, high oscillating core inlet mass flow rate was predicted between 100 and 200 s. This high mass flow rate seems to result in the underestimation of the turnaround temperatures.

The agreement of TRAC results with CCTF result is not so bad for the turnaround behavior of heater rods in the core. The turnaround of heater rods predicted in the period that the overestimation of downcomer-to-core U-tube-type oscillation is predicted in the TRAC calculation. It can be corsidered that the oscillations disturb the accuracy of the core cooling prediction. Therefore, a review of the oscillations is recommended again to improve the capability of the TRAC code for the prediction of the turnaround behavior of heater rods or fuel rods.

Figure 22 shows the comparison of the quench time. The TRAC results show excellent agreement with the test results in all power regions except for the upper part of the heater rods.

4.4 Summary of data comparisons

The results of TRAC-PD2 post-test analysis for the CCTF Evaluation Model Test C1-19 (Run 38) were compared with the CCTF test results component-by-component in the previous sections. In the system calculation, the calculation results of each component is coupled such that it is difficult to identify the main problem in the modeling.
In this section, the problems in the TRAC calculation are summarized by rearranging the results from data comparisons in order of time sequence.

(1) In the early period of the reflood (between 102 and 200 s), TRAC overestimates the downcomer-to-core U-tube-type oscillations. This results in a higher core inlet fluid temperature, the overestimation of the spill-over water mass through the break and the

underestimation of the water mass accumulated in the core in the period. The accuracy of the TRAC prediction for the turnaround behavior of heater rods was not so good because of these discrepancies in the hydraulic behavior. A review is recommended for the core hydraulic model in the early period of the reflood.

(2) In the later period of the reflood (after 200 s), the time-averaged core inlet mass flow rate showed excellent agreement with the test result. TRAC overestimated the core water accumulation rate and underestimated the vented mass flow rate through the four primary loops. These errors were cancelled as described by Eq. (2). Excellent agreement in the core inlet mass flow rate with CCTF result was obtained in the TRAC calculation after 200 s. However, these facts still suggest the need for future improvement of the core hydraulics concerned with water accumulation.

(3) For the loop thermohydraulic behavior, TRAC overestimated the loop flow resistance coefficient by 65 percent and underestimated the heat transfer from the secondary side to the primary side of the steam generator. It was found that the underestimation of the heat transfer in the steam generator was caused mainly by the error in the estimation of the carry-over from the upper plenum to the hot leg. A separate calculation of the steam generator heat transfer is recommended and a review for the carry-over from the upper plenum is also recommended to improve the estimation error of the loop thermal-hydraulic behavior in the TRAC calculation.

5. MULTIDIMENSIONAL BEHAVIOR IN TRAC CALCULATION

5.1 Core Hydraulic Behavior

Figures 23 (a) and (b) show the time-averaged superficial velocities of steam and water in the core, respectively. To get the superficial velocities, the predicted mass flow rates were averaged with a sampling rate of 10 Hz from the calculational output between 300 and 500 s. The mass flow rates were integrated with a trapezoid formula. The integrated results are shown in Appendix A. The mean slope of each curve in Appendix A represents the time-averaged mass flow rate. The mean slopes between 300 and 500 s were used to determine Fig. 23.

underestimation of the water mass accumulated in the core in the period. The accuracy of the TRAC prediction for the turnaround behavior of heater rods was not so good because of these discrepancies in the hydraulic behavior. A review is recommended for the core hydraulic model in the early period of the reflood.

(2) In the later period of the reflood (after 200 s), the time-averaged core inlet mass flow rate showed excellent agreement with the test result. TRAC overestimated the core water accumulation rate and underestimated the vented mass flow rate through the four primary loops. These errors were cancelled as described by Eq. (2). Excellent agreement in the core inlet mass flow rate with CCTF result was obtained in the TRAC calculation after 200 s. However, these facts still suggest the need for future improvement of the core hydraulics concerned with water accumulation.

(3) For the loop thermohydraulic behavior, TRAC overestimated the loop flow resistance coefficient by 65 percent and underestimated the heat transfer from the secondary side to the primary side of the steam generator. It was found that the underestimation of the heat transfer in the steam generator was caused mainly by the error in the estimation of the carry-over from the upper plenum to the hot leg. A separate calculation of the steam generator heat transfer is recommended and a review for the carry-over from the upper plenum is also recommended to improve the estimation error of the loop thermal-hydraulic behavior in the TRAC calculation.

5. MULTIDIMENSIONAL BEHAVIOR IN TRAC CALCULATION

5.1 Core Hydraulic Behavior

Figures 23 (a) and (b) show the time-averaged superficial velocities of steam and water in the core, respectively. To get the superficial velocities, the predicted mass flow rates were averaged with a sampling rate of 10 Hz from the calculational output between 300 and 500 s. The mass flow rates were integrated with a trapezoid formula. The integrated results are shown in Appendix A. The mean slope of each curve in Appendix A represents the time-averaged mass flow rate. The mean slopes between 300 and 500 s were used to determine Fig. 23.

The quench front shown in Fig. 23 is for the medium power rod in the medium power region and it propagates from 1.4 m to 2.4 m during the previously-mentioned averaging period of the mass flow rates. Below the quench front, water goes down in the outer ring (low power region) of the core and it goes up in the inner ring (high power region). It can be considered that the water flow, from the outer ring to the inner ring, is predicted in the fluid cells between 0.0 and 0.305 m and that the radial water flow causes the increase of the axial component of the water velocity in the inner cells at the bottom part of the core. Near the quench front, a significant velocity change occurs in the TRAC calculation. The velocity change can be attributed to the water accumulation below the quench front, the steam generation at the quench front and the radial water velocity from the inner cell to the outer cell resulting in the downward water flow in the outer ring. TRAC predicts the water circulation below the quench front. Above the quench front, no significant circulation was calculated to occur.

The superficial steam velocity increases with the elevation and it shows no downward flow in the core. Below the quench front, the steam velocity is higher in the inner ring (higher power region) than in the outer ring (lower power region), while almost equal steam velocities are predicted just above the quench front (at the elevation of 2.745 m). This suggests steam flow in the radial direction from the inner ring to the outer ring at the quench front. At the exit of the core, the higher steam velocity in the inner ring is established again. This redistribution of the steam velocity may be caused by the interaction with the fluid in the upper plenum.

The flow distribution in the core should depend on the input parameters such as the hydraulic diameters, the flow areas at each cell boundary. We have no available test data to compare with the predicted results so that the sensitivity studies on the input data are recommended to get more information on the multidimensional flow behavior.

5.2 Downcomer Hydraulic Behavior

Table 4 shows the comparison of the overall mass balance relation at the top of the downcomer between the CCTF and TRAC results. All data shows the time-averaged mass flow rate between 300 and 500 s in unit of kg/s. The water inflow m_I^* and the steam inflow m_{gI}^* from the intact cold

legs to downcomer was estimated assuming the thermal equilibrium in the cold legs using the measured steam mass flow rate from the steam generator m_{gI} and the ECC water injection rate m_{ECC}. The steam generation rate in the downcomer m_{gD} was assumed to be equal to the TRAC code calculated value in the CCTF results. The vented steam mass flow rate through the broken cold leg m_{gB} and the water downward flow in the downcomer m_D was calculated using the equations shown in Table 4.

TRAC result shows good agreement for the water inflow from intact cold legs with CCTF result. The steam inflow from intact cold legs is about half of the CCTF result in the TRAC calculation because of the underestimation of the steam mass flow rate from the steam generator. The steam outflow through the broken cold leg is also about half of the CCTF result in the TRAC calculation. The water outflow through the broken cold leg is higher by 0.66 kg/s than CCTF result in the TRAC calculation. The downward water flow into the lower part of the downcomer in the TRAC calculation is lower by about 1 kg/s than the CCTF results. Even though the TRAC results show some discrepancies quantitatively, it can be considered that TRAC results show reasonable agreement with the CCTF results for the mass balance at the top of the downcomer.

Figure 24 shows the axial components of the superficial velocities of steam and water in the downcomer. Figure 25 shows the time-averaged component in the azimuthal direction of the downcomer. All data are based on the time averaged mass flow rate between 300 and 500 s. The annulus of the downcomer was unfolded into the plane in Fig. 24. A cold leg of each of the four primary loops was connected to each of the four cells at the fifteenth axial level (between 6.96 and 7.4 m). The broken loop was connected to the first azimuthal sector (θ = 1).

In Fig. 25, high circumferential mass flow to the broken cold leg is predicted over the cold leg level for steam. For water, high circumferential mass flow to the broken cold leg is predicted below the cold leg level. In Fig. 24, the steam velocity at the elevation of 7.4 m shows high upward steam flow for the fluid cells connected to the intact cold legs, while the water velocity at the elevation of 6.96 m shows high downward water flow for these fluid cells. These results suggest that water from the intact cold legs flows to the broken cold leg by way of the lower cells and that steam from the intact cold legs flows to the broken cold leg by way of the upper cells. TRAC results

suggest the phase separation of the two phase mixture from the intact cold legs at the top of the downcomer.

Figure 25 shows that the water, which is not overflowed through the broken cold leg, flows downward through the first and second azimuthal sectors and that the upward water flow occurs at the lower half of the third and fourth azimuthal sectors. It is uncertain at present why these water flow distributions were predicted in the TRAC calculation.

There are no measured data to compare with the predicted results for the multidimensional flow behaviors in the downcomer. Sensitivity studies are recommended to get more information on the multi-dimensional flow behaviors.

5.3 Upper Plenum Hydraulic Behavior

Figure 26 shows the superficial velocity of the steam and water in the upper plenum. All velocities represent the time-averaged values between 300 and 500 s. The circulation of the water is predicted between the hot leg and the top of the core. The water velocity at 1.2 m above the upper core support plate (UCSP) is almost equal to zero. This indicates that almost all the water is de-entrained in the upper plenum and that the carry-over to the hot leg is nearly equal to zero. As mentioned in previous section, this result is not consistent with the CCTF test results.

Asymmetric flow distributions are predicted for both steam and water in the upper plenum. Again, no experimental data exists to assess this hydraulic behavior and sensitivity studies are recommended to study the de-entrainment phenomena and to get more information on the multi-dimensional flow behavior in the upper plenum.

6. CONCLUSIONS AND RECOMMENDATIONS

The results of TRAC-PD2 post-test analysis for the CCTF Evaluation Model Test (Run 38) were analyzed to assess the capability of the TRAC code for the prediction of the thermal-hydraulic behavior during a loss-of-coolant accident of a pressurized water reactor. Through the comparisons with CCTF test results, it was found that the accuracy of the TRAC prediction of the turnaround behavior of heater rods was decreased

suggest the phase separation of the two phase mixture from the intact cold legs at the top of the downcomer.

Figure 25 shows that the water, which is not overflowed through the broken cold leg, flows downward through the first and second azimuthal sectors and that the upward water flow occurs at the lower half of the third and fourth azimuthal sectors. It is uncertain at present why these water flow distributions were predicted in the TRAC calculation.

There are no measured data to compare with the predicted results for the multidimensional flow behaviors in the downcomer. Sensitivity studies are recommended to get more information on the multi-dimensional flow behaviors.

5.3 Upper Plenum Hydraulic Behavior

Figure 26 shows the superficial velocity of the steam and water in the upper plenum. All velocities represent the time-averaged values between 300 and 500 s. The circulation of the water is predicted between the hot leg and the top of the core. The water velocity at 1.2 m above the upper core support plate (UCSP) is almost equal to zero. This indicates that almost all the water is de-entrained in the upper plenum and that the carry-over to the hot leg is nearly equal to zero. As mentioned in previous section, this result is not consistent with the CCTF test results.

Asymmetric flow distributions are predicted for both steam and water in the upper plenum. Again, no experimental data exists to assess this hydraulic behavior and sensitivity studies are recommended to study the de-entrainment phenomena and to get more information on the multi-dimensional flow behavior in the upper plenum.

6. CONCLUSIONS AND RECOMMENDATIONS

The results of TRAC-PD2 post-test analysis for the CCTF Evaluation Model Test (Run 38) were analyzed to assess the capability of the TRAC code for the prediction of the thermal-hydraulic behavior during a loss-of-coolant accident of a pressurized water reactor. Through the comparisons with CCTF test results, it was found that the accuracy of the TRAC prediction of the turnaround behavior of heater rods was decreased

due to the overestimation of the downcomer-to-core U-tube-type oscillation in the early period of the reflood (before 200 s in the CCTF test). For the later period of the reflood (after 200 s in the CCTF test), TRAC overestimated the core water accumulation rate and underestimated the carry-over from the upper plenum to the primary loops, the loop mass flow rate; and the heat transfer from the secondary side to the primary side of the steam generator. However, these errors cancelled each other in the TRAC calculation and allowed excellent agreement of the core inlet mass flow rate and the quench time of heater rods in the later period of the reflood. As a summary of data comparisons, a review was recommended for the hydraulic model in the vessel to clarify why TRAC overestimates the downcomer-to-core U-tube-type oscillation in the early period of the reflood, the hydraulic model in the vessel to clarify why TRAC overestimates the water accumulation rate in the core and underestimates the water carry-over to the primary loops.
A separate calculation for the loop thermal-hydraulic behavior in the CCTF test was also recommended to improve the loop flow resistance model and the steam generator heat transfer model in the TRAC code.

The predicted flow behavior in the pressure vessel was surveyed on a time averaged basis. TRAC results showed asymmetric velocity profiles in the core, the downcomer and the upper plenum. TRAC results suggested that the multidimensional effect was not negligible in the CCTF. However, the reliability of the TRAC prediction is uncertain at present because there was no experimental basis for the multidimensional flow in the CCTF test. A sensitivity study with TRAC is recommended to get more information on the multidimensional flow behavior in the CCTF tests. It is necessary to study more in order to clarify the effect of the multidimensional flow behavior both experimentally and analytically.

ACKNOWLEDGMENTS

This work was performed during the stay at Los Alamos National Laboratory (LANL) where the author was delegated as a resident engineer in the 2D/3D program since February 1982 to March 1983. He would like to thank Dr. K. Williams, Messrs. R. Fujita, M. Cappiello and Mrs. S. Smith of Los Alamos National Laboratory for their helpful advice. Grateful thanks are forwarded to Mr. F. Motley, who performed the TRAC calculation, for providing support and valuable discussions.

He would like to express his thanks to Dr. M. Nozawa, Deputy Director General of Tokai Research Establishment JAERI, Dr. S. Katsuragi, Director of Reactor Safety Research Center of JAERI, Dr. M. Ishikawa, Director of Department of Nuclear Safety Evaluation, Dr. M. Hirata, Director of Department of Nuclear Safety Research, Dr. K. Hirano, Deputy Director of Nuclear Safety Research, and Dr. Y. Murao, General Manager of Reactor Safety Laboratory II, for their guidance and encouragement.

He also appreciates to the members of the CCTF analysis group, Messrs. T. Iguchi, T. Sudoh, J. Sugimoto and T. Okubo for valuable discussions.

REFERENCES

1. MURAO, Y., et al.: "Experimental study of system behavior during reflood of PWR-LOCA using CCTF", J. Nucl. Sci. and Technol., 19(9), pp. 705-719, (1982).
2. LILES, D., et al.: "TRAC-PD2: An Advanced Best-Estimate Computer Program for Pressurized Water Reactor Loss-of-Coolant Accident Analysis", LA-8709-MS, NUREG/CR-2054, (1981).
3. KIRCHNER, W. L. and WILLIAMS, K. A.: "FY 1981 2D/3D Analysis Program Annual Report", LA-2D/3D-TN-81-36, (1982).
4. MOTLEY, F.: "Investigation of Radial Power and Temperature Effects in Large-Scale Reflood Experiments", Proceeding of Second International Topical Meeting on Nuclear Reactor Thermal Hydraulics", January, (1983).
5. MURAO, Y., et al.: "Evaluation Report on CCTF Core-I Reflood Test C1-19 (Run 38)", JAERI-M 83-029, February (1983).

ACKNOWLEDGMENTS

This work was performed during the stay at Los Alamos National Laboratory (LANL) where the author was delegated as a resident engineer in the 2D/3D program since February 1982 to March 1983. He would like to thank Dr. K. Williams, Messrs. R. Fujita, M. Cappiello and Mrs. S. Smith of Los Alamos National Laboratory for their helpful advice. Grateful thanks are forwarded to Mr. F. Motley, who performed the TRAC calculation, for providing support and valuable discussions.

He would like to express his thanks to Dr. M. Nozawa, Deputy Director General of Tokai Research Establishment JAERI, Dr. S. Katsuragi, Director of Reactor Safety Research Center of JAERI, Dr. M. Ishikawa, Director of Department of Nuclear Safety Evaluation, Dr. M. Hirata, Director of Department of Nuclear Safety Research, Dr. K. Hirano, Deputy Director of Nuclear Safety Research, and Dr. Y. Murao, General Manager of Reactor Safety Laboratory II, for their guidance and encouragement.

He also appreciates to the members of the CCTF analysis group, Messrs. T. Iguchi, T. Sudoh, J. Sugimoto and T. Okubo for valuable discussions.

REFERENCES

1. MURAO, Y., et al.: "Experimental study of system behavior during reflood of PWR-LOCA using CCTF", J. Nucl. Sci. and Technol., 19(9), pp. 705-719, (1982).
2. LILES, D., et al.: "TRAC-PD2: An Advanced Best-Estimate Computer Program for Pressurized Water Reactor Loss-of-Coolant Accident Analysis", LA-8709-MS, NUREG/CR-2054, (1981).
3. KIRCHNER, W. L. and WILLIAMS, K. A.: "FY 1981 2D/3D Analysis Program Annual Report", LA-2D/3D-TN-81-36, (1982).
4. MOTLEY, F.: "Investigation of Radial Power and Temperature Effects in Large-Scale Reflood Experiments", Proceeding of Second International Topical Meeting on Nuclear Reactor Thermal Hydraulics", January, (1983).
5. MURAO, Y., et al.: "Evaluation Report on CCTF Core-I Reflood Test C1-19 (Run 38)", JAERI-M 83-029, February (1983).

Table 1 Summary of test conditions

1. Test type : Evaluation Model Test
2. Test number : Run 038 3. Date : March 18, 1981
4. Power : Total: 9.28 MW; Linear: 1.39 kW/m
5. Radial power shape :

   Zone: A B C

   Ratio: 1.299 1.092 0.841
6. Axial power shape : Chopped cosine
7. Pressure (MPa) :

   System: 0.20, Containment 0.20,

   Steam generator secondary: 5.21
8. Temperature (K) :

   Downcomer wall 442, Vessel internals 388,

   Primary piping wall 396, Lower plenum liquid 387,

   ECC Liquid 311, Steam generator secondary 536,

   Peak clad temperature at ECC initiation 1117
9. ECC injection

   Lower plenum + cold leg
10. Pump K-factor : ∿ 15
11. ECC flow rates and duration :

    Accumulator 0.103 m^3/s from 0 to 25.5 s

    LPCI 0.0113 m^3/s from 25.5 to 737 s

    ECC injection to lower plenum : from 0 to 14 s

    (Valve opening and closing times are included in the injection duration)
12. Initial water level in lower plenum : 0.89 M.
13. Power control : ANS × 1.2 + Actinide (30 s after scram)
14. Expected BOCREC time from ECC initiation 9 s
15. Expected peak temperature at reflood initiation 1143 K

Table 2 Comparison of the time-averaged core inlet mass flow rate between CCTF and TRAC results

(a) CCTF

Item*1	Time (s)		Time averaged mass flow rate*2 (kg/s)
	300	500	
M_{CR} (kg)	411.62	392.95	-0.09
M_{UP} (kg)	101.50	139.70	0.19
M_L (kg)	959.07	1871.40	4.56
M_F (kg)	1472.19	2404.05	4.66

(b) TRAC

Item*1	Time (s)		Time averaged mass flow rate*2 (kg/s)
	300	500	
M_{CR} (kg)	310.0	394.0	0.42
M_{UP} (kg)	19.91	70.81	0.26
M_L (kg)	753.17	1522.22	3.85
M_F (kg)	1100.0	2040.	4.70

Note (*1) M_F : Total core inlet mass flow (kg).

M_{CR} : Core liquid mass (kg).

M_{UP} : Upper plenum liquid mass (kg).

M_L : Total vented mass through the four primary loops (kg).

(*2) $m_x = [M_x (500\ s) - M_x (300\ s)]/200$

Table 3 Comparison between TRAC and CCTF results of the sectional differential pressure along the intact loop 2

Items	TRAC	CCTF	Difference
D/P through hot leg (kPa)	0.23	3.00	-2.77
D/P through steam generator (kPa)	7.23	3.26	+3.97
D/P through loop seal (kPa)	1.82	1.87	-0.05
D/P through pump orifice (kPa)	13.80	13.97	-0.17
D/P through cold leg (kPa)	4.10	-0.37	+4.47
D/P through the intact loop 2 (kPa)	27.20	21.72	+5.48
Mass flow rate through hot leg (kg/s)	0.843	1.047	-0.204

Note : The time-averaged values between 300 and 500 s are shown in the table.
D/P: Differential Pressure

Table 4 Comparison of the mass flow rate at the top of the downcomer

	Intact Cold Leg				Downcomer			Broken Cold Leg	
(*6) (kg/s)	m_{gI}	m_{ECC}	m^*_I	m^*_{gI}	m_{gD}	m_D	m_{DC}	m_B	m_{gB}
TRAC	2.52	11.10	13.01 (*2)	0.61 (*2)	0.05	4.14	0.23	8.64	0.66 (*4)
CCTF	3.08 (*1)	11.25 (*1)	13.01 (*2)	1.32 (*2)	0.05 (*3)	5.03 (*5)	0.00 (*1)	7.98 (*1)	1.37 (*4)

NOTE: All are time averaged value between 300 and 500 s.

(*1) Measured value.

(*2) Evaluated value with the assumption of the equilibrium in the cold leg.

(*3) CCTF value is assumed to equal to the predicted value by the TRAC code.

(*4) $m_{gB} = m_{gD} + m^*_{gI}$

(*5) $m_D = m^*_I - m_B - m_{DC}$

(*6) nomenclature

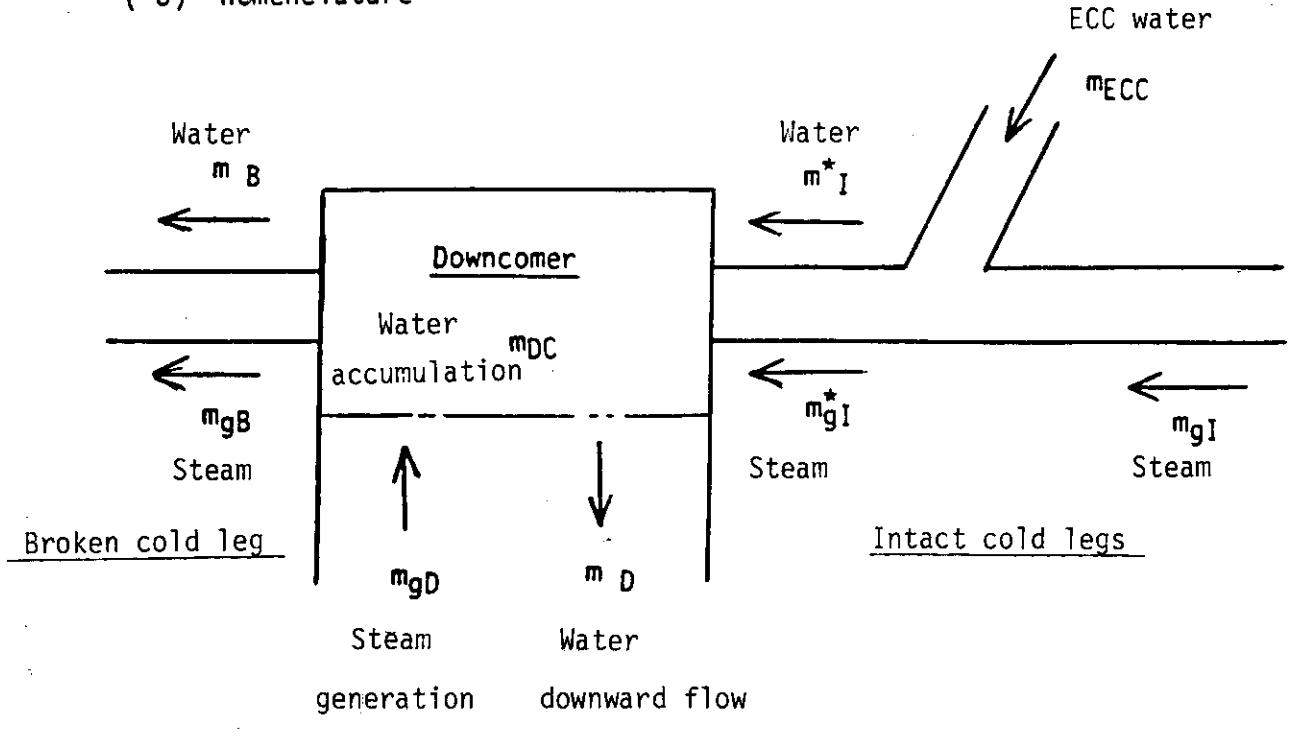

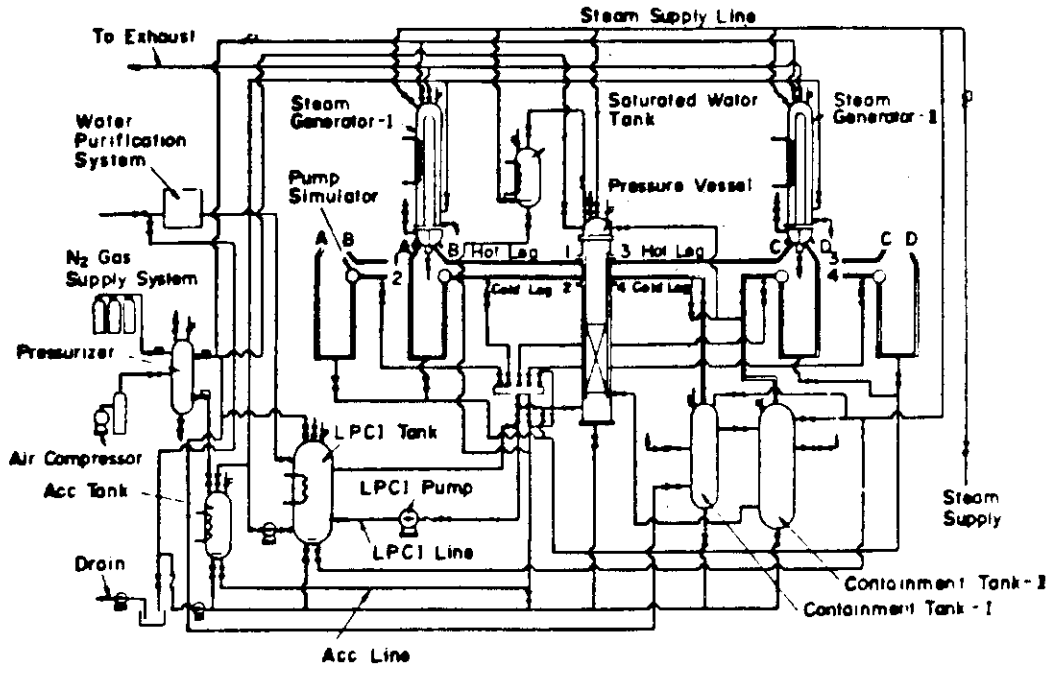

Fig. 1 Schematic diagram of the Cylindrical Core Test Facility.

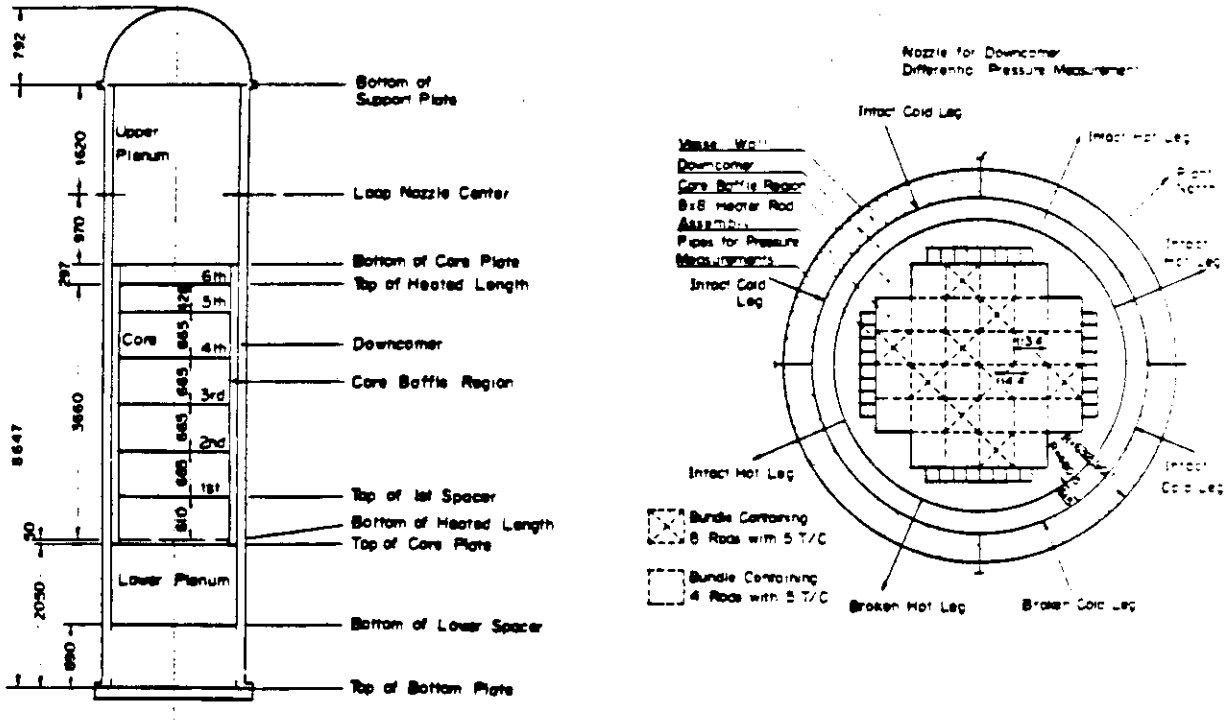

Fig. 2 Dimensions of the pressure vessel.

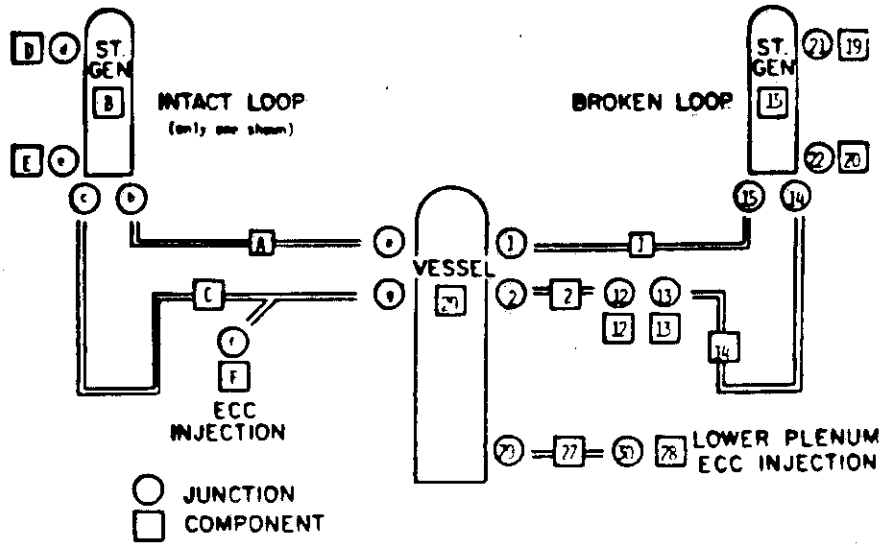

Fig. 3 TRAC noding schematic for CCTF.

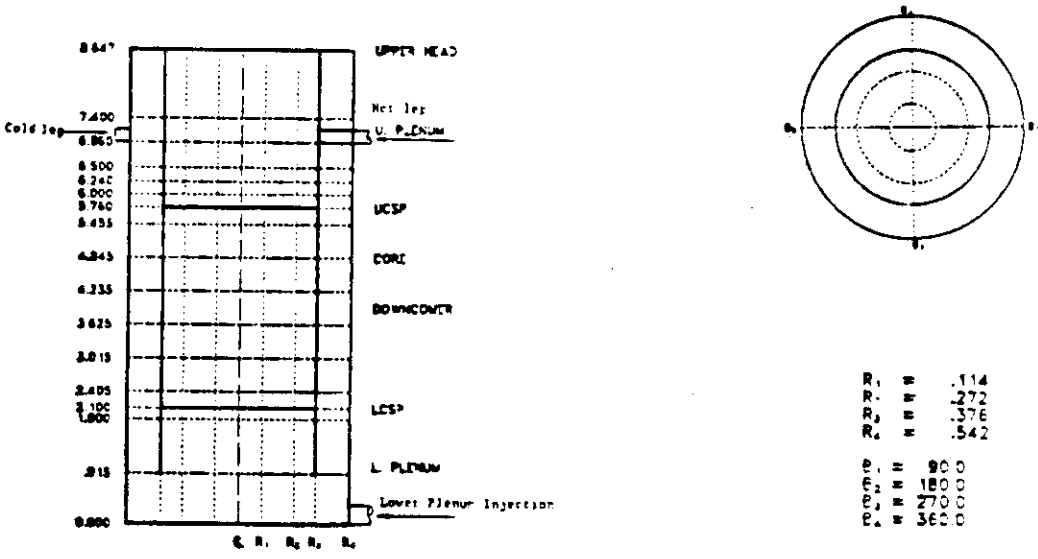

Fig. 4 TRAC noding schematic for the vessel of the fine node model.

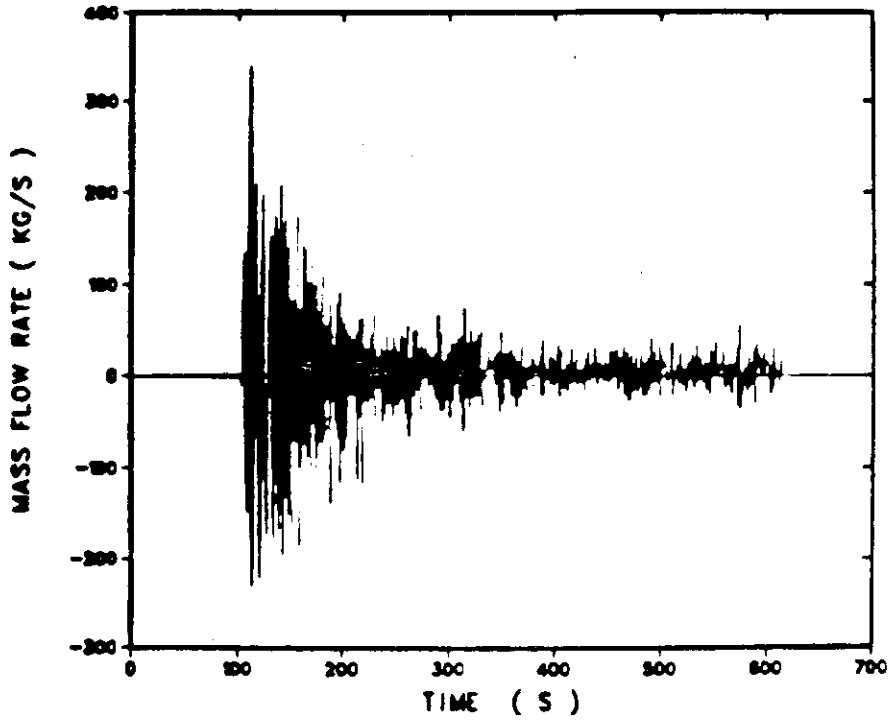

Fig. 5 Predicted core inlet mass flow rate.

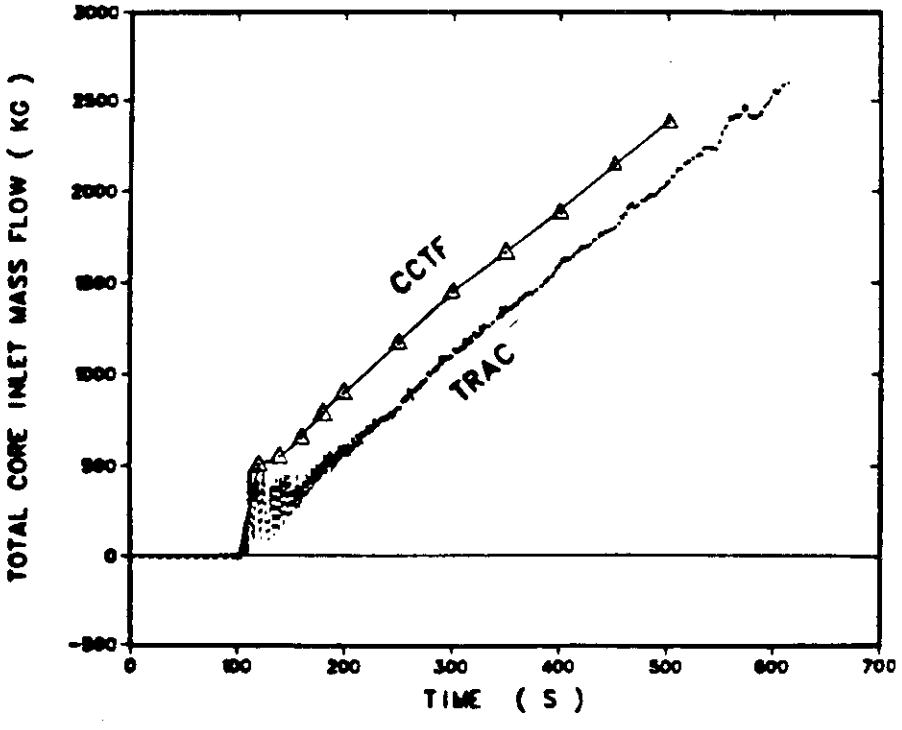

Fig. 6 Comparison of the total core inlet mass flow.

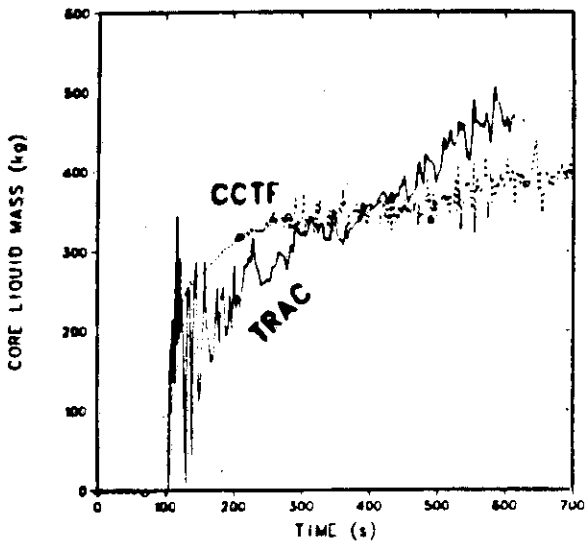

CORE LIQUID MASS

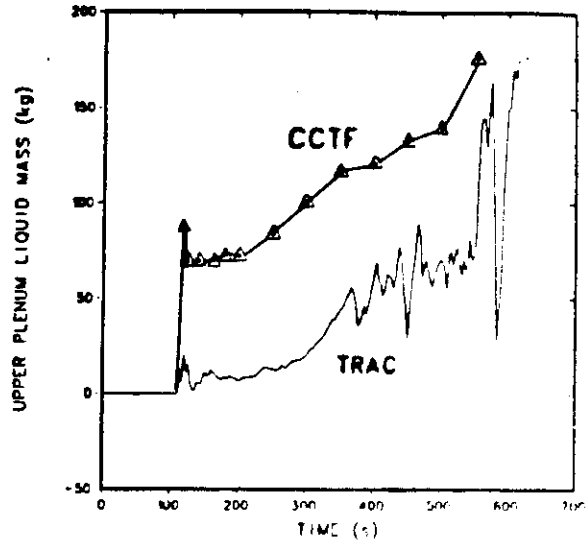

UPPER PLENUM LIQUID MASS

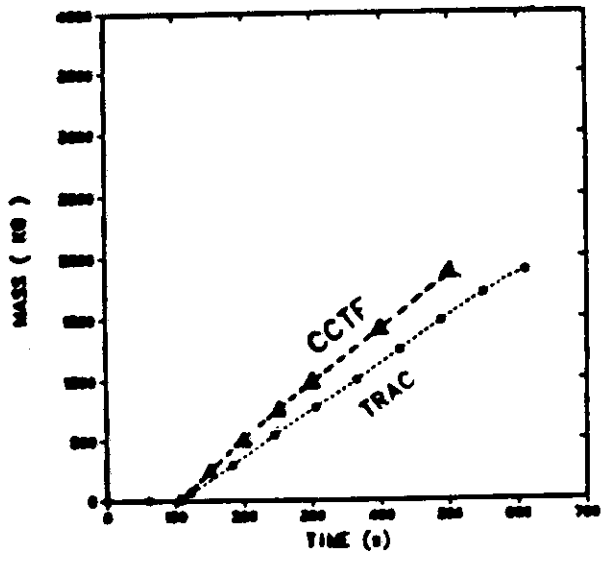

VENTED MASS THROUGH LOOPS

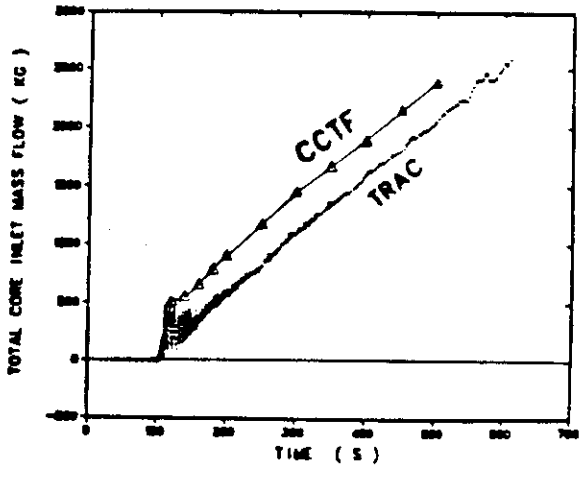

TOTAL CORE INLET MASS FLOW

Fig. 7 Comparison of the core liquid mass, the upper plenum mass, the vented mass through the four primary loops and the total core inlet mass flow.

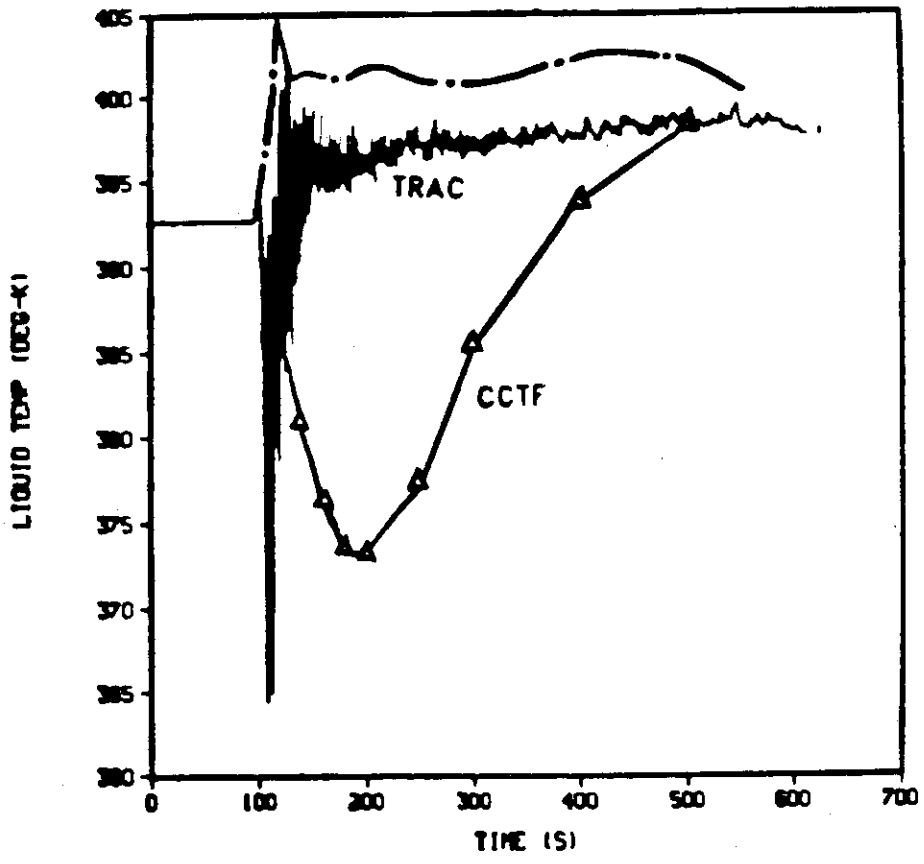

Fig. 8 Comparison of fluid temperature at the core inlet.

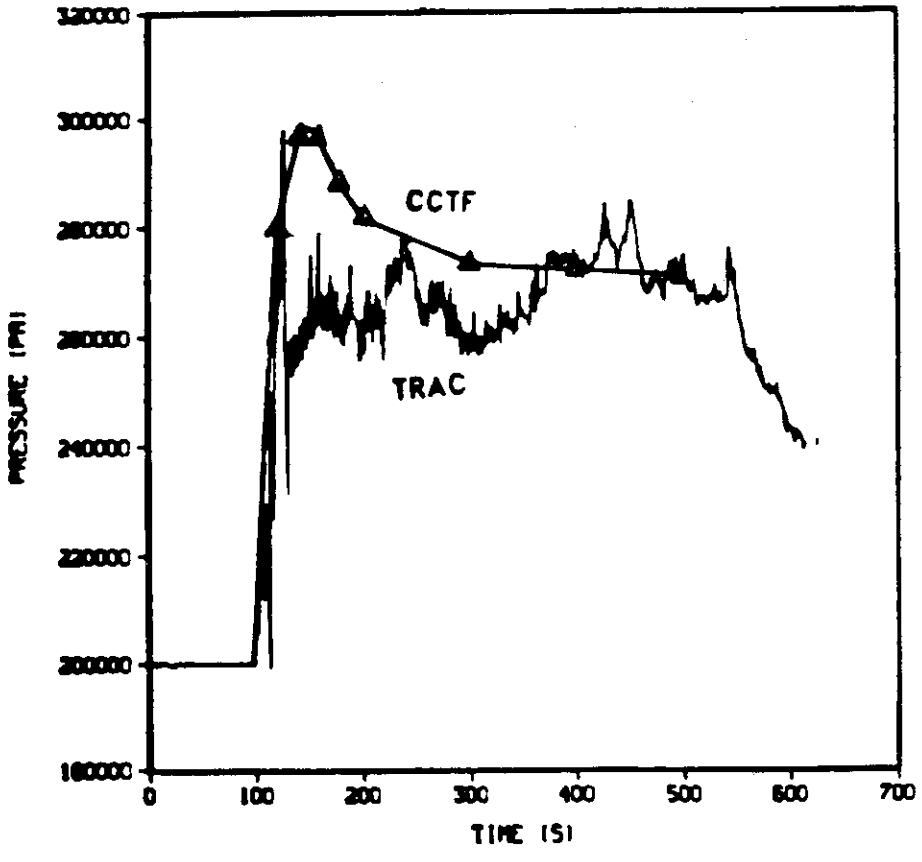

Fig. 9 Comparison of core inlet pressure.

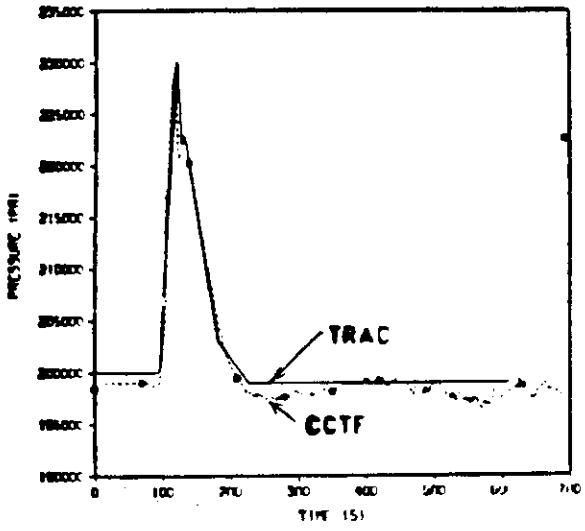

P_{CN} : containment pressure

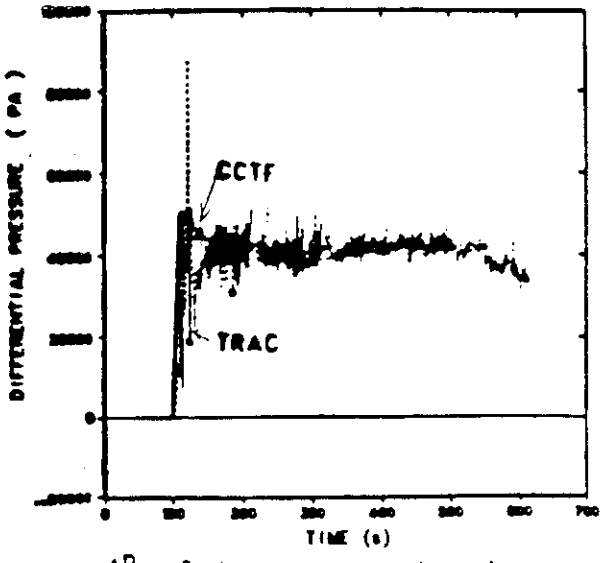

ΔP_D : downcomer water head

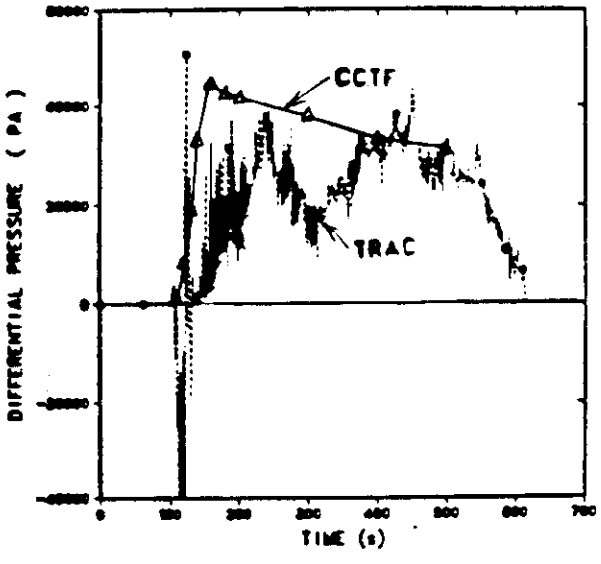

ΔP_{BCL} : pressure drop through the broken cold leg

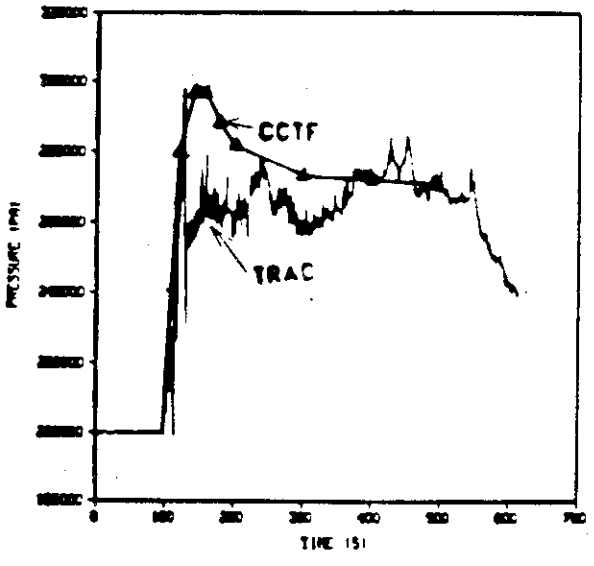

P_{CR} : core inlet pressure

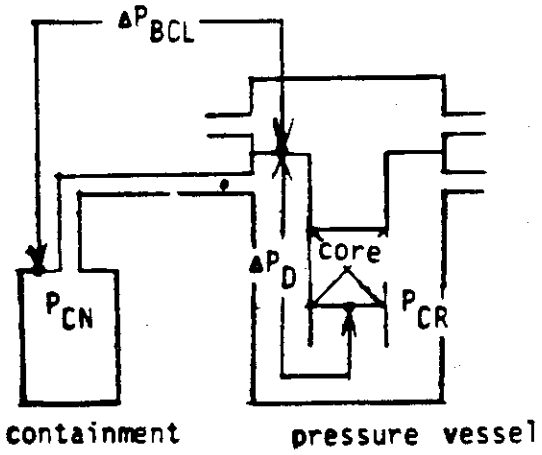

$$P_{CR} = P_{CN} + \Delta P_{BCL} + \Delta P_D$$

P_{CR} : core inlet pressure

P_{CN} : containment pressure

ΔP_{BCL} : pressure drop through the broken cold leg

ΔP_D : downcomer water head

Fig. 10 Comparison of P_{CR}, P_{CN}, ΔP_{BCL}, and ΔP_D

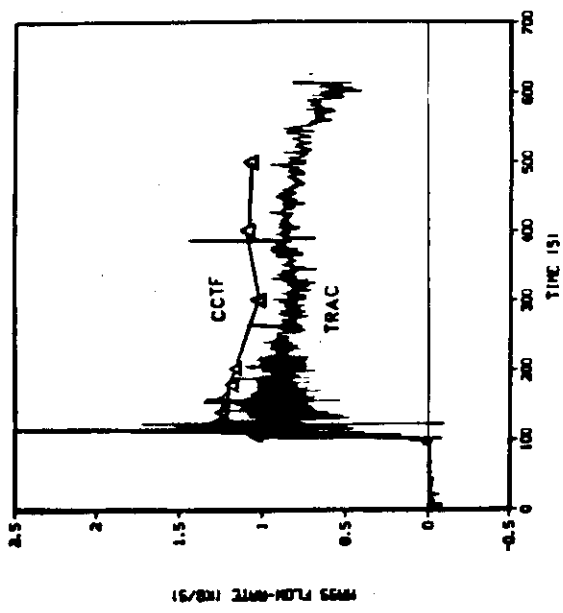

Fig. 13 Comparison of the mass flow rate and the total pressure drop through an intact loop.

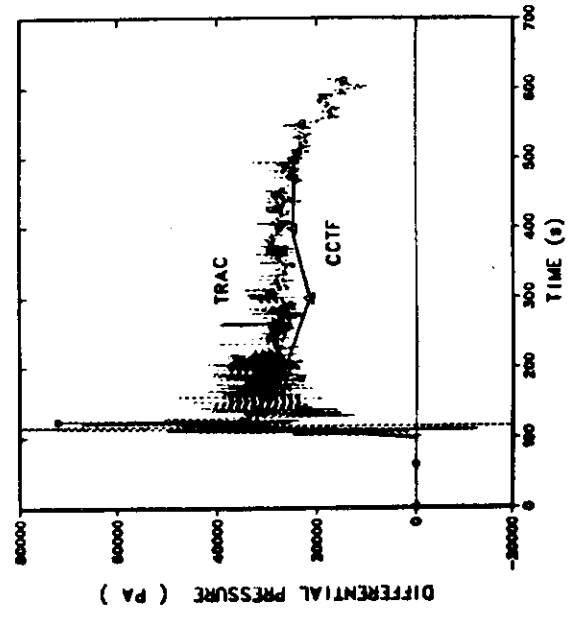

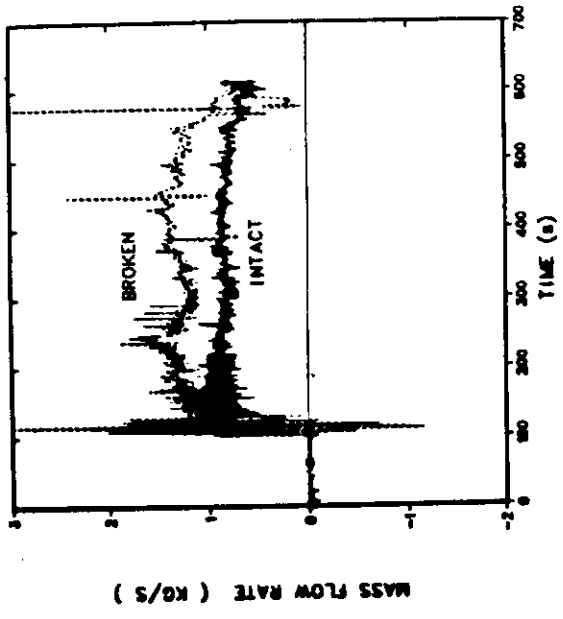

Fig. 11 Predicted mass flow rate through intact and broken loops.

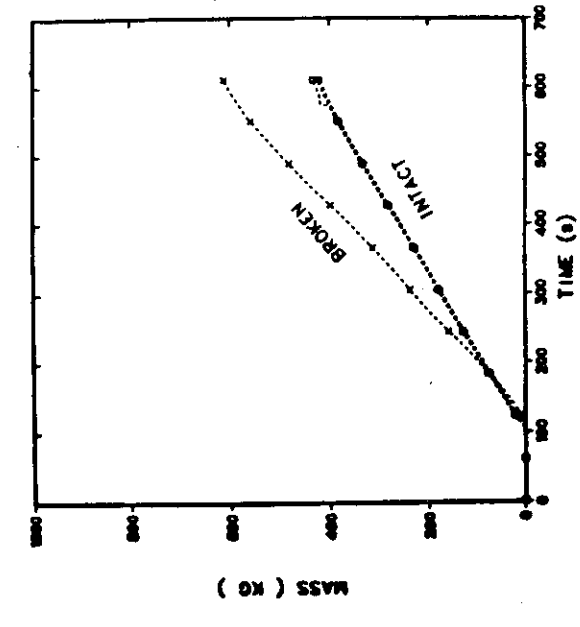

Fig. 12 Predicted total mass flow through intact and broken loops.

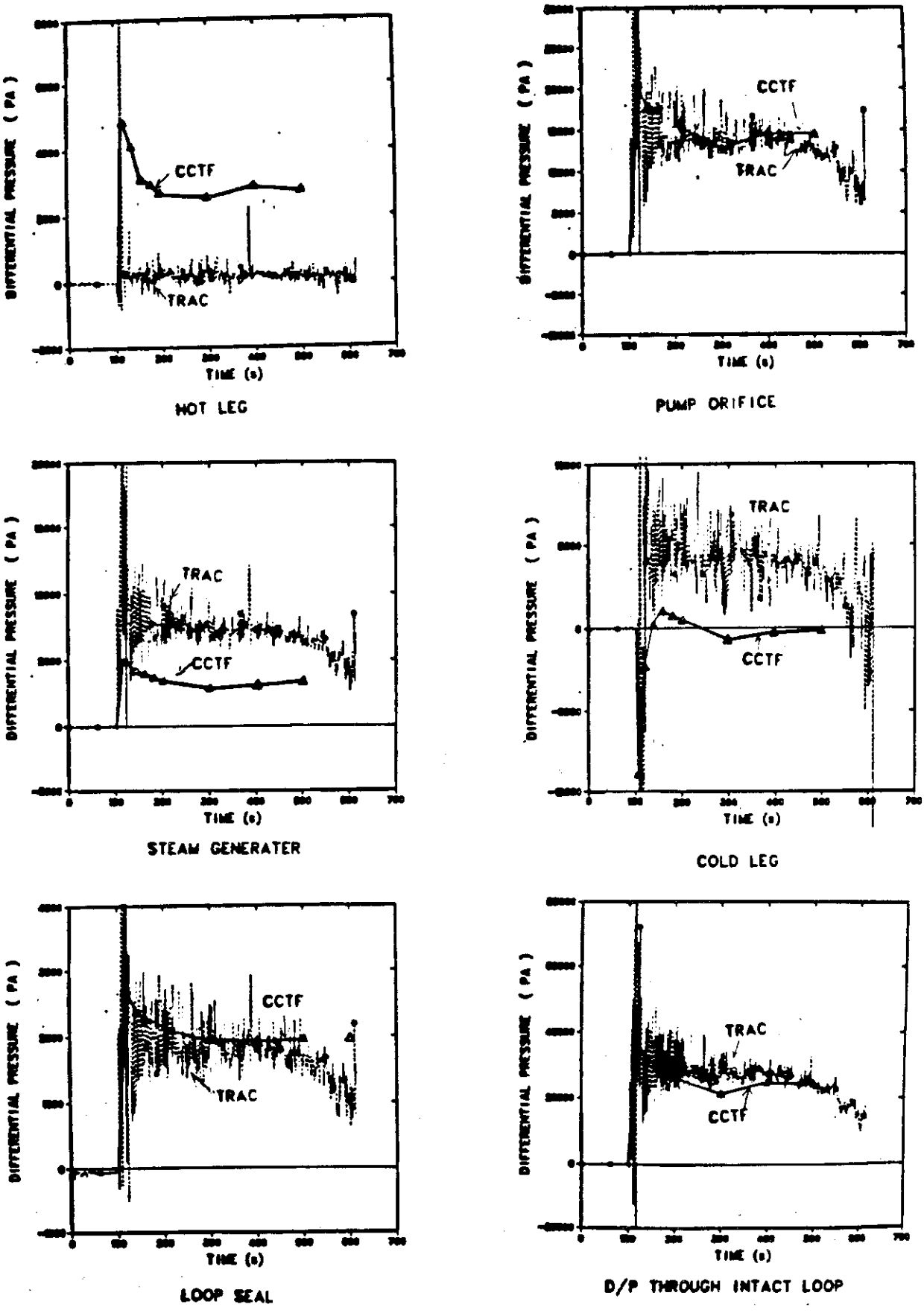

Fig. 14 Comparison of the component-by-component differential pressure for the intact loop.

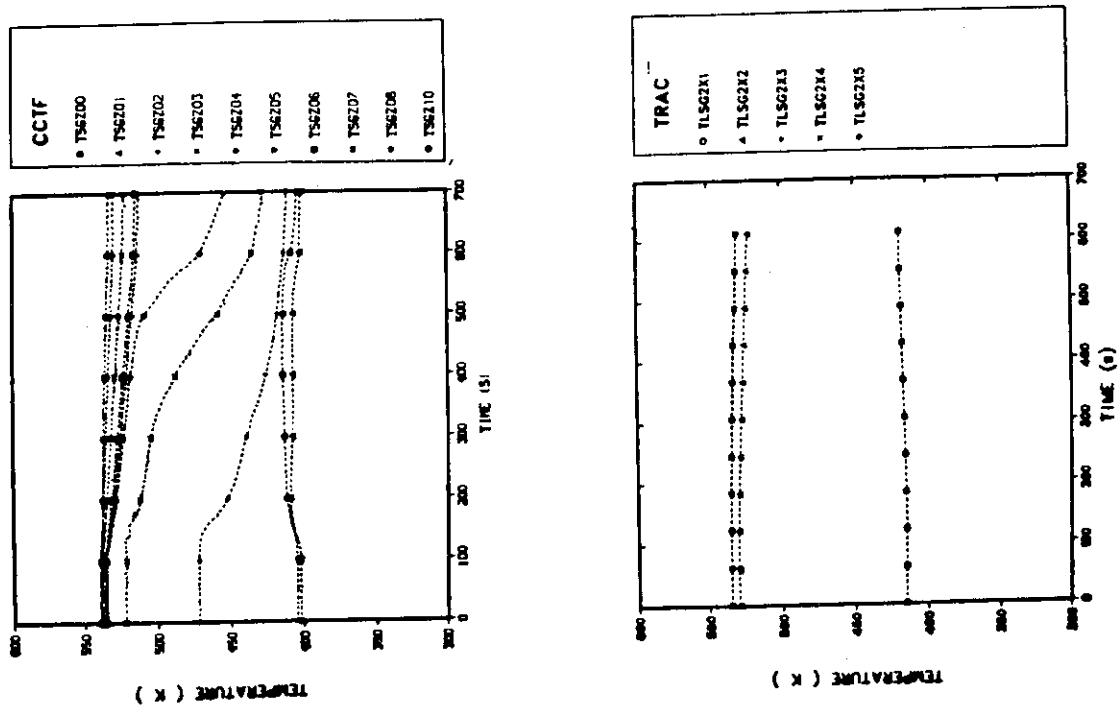

Fig. 16 Comparison of the fluid temperature in the secondary side of the steam generator.

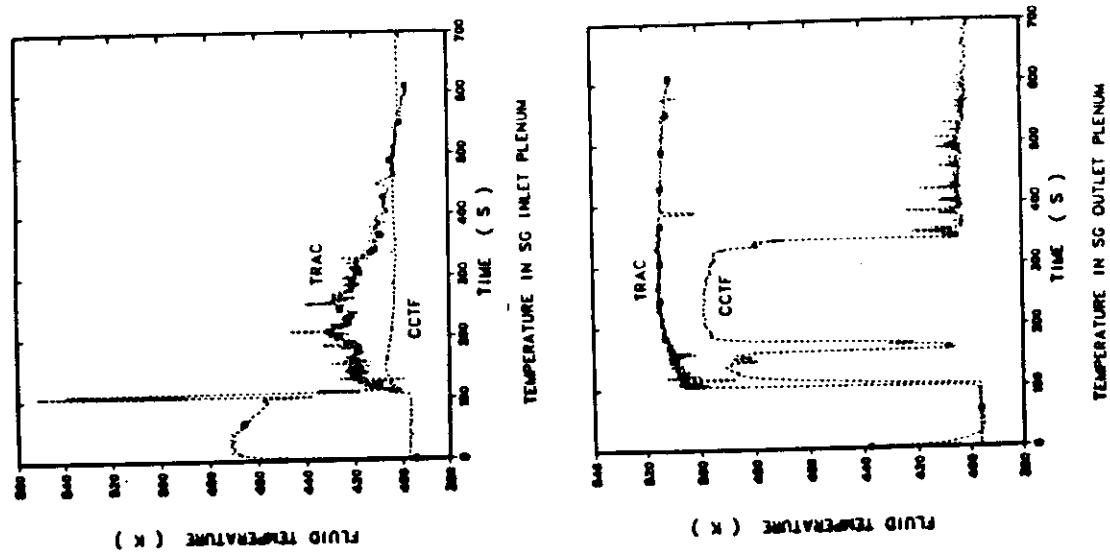

Fig. 15 Comparison of the fluid temperature at the inlet and outlet plenums of the steam generator.

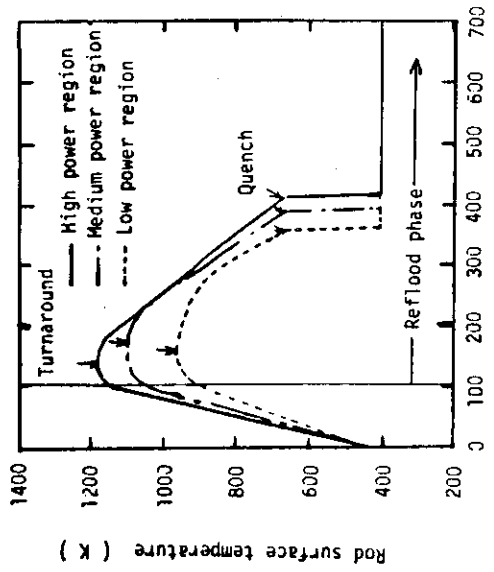

(a) C C T F

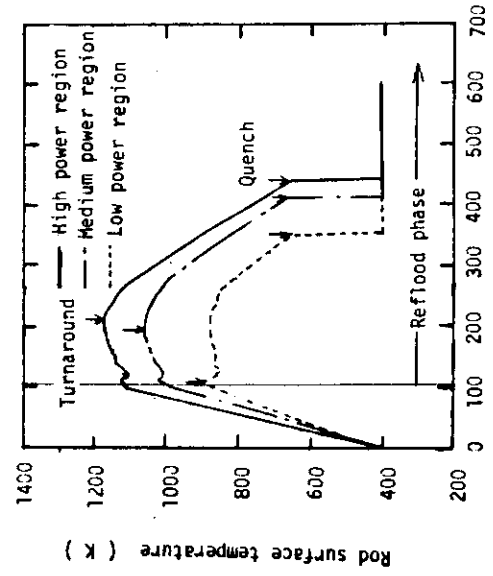

(b) T R A C

Fig. 19 Comparison of the rod surface temperature at the midplane of the medium power rod in the high (radial peaking factor P_R = 1.299), medium (P_R = 1.092) and low (P_R = 0.841) power regions.

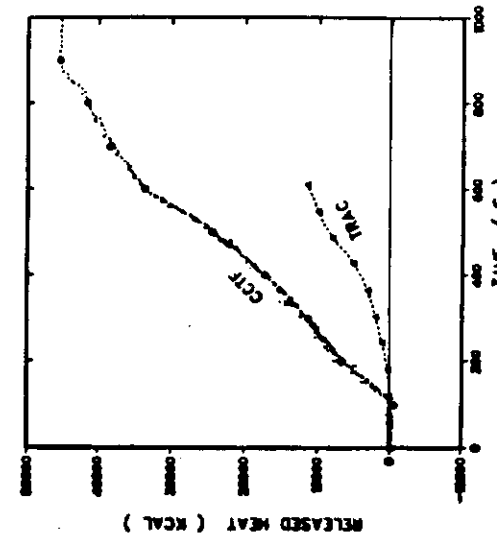

Fig. 17 Comparison of the total energy transferred from the secondary side to the primary side of the steam generator.

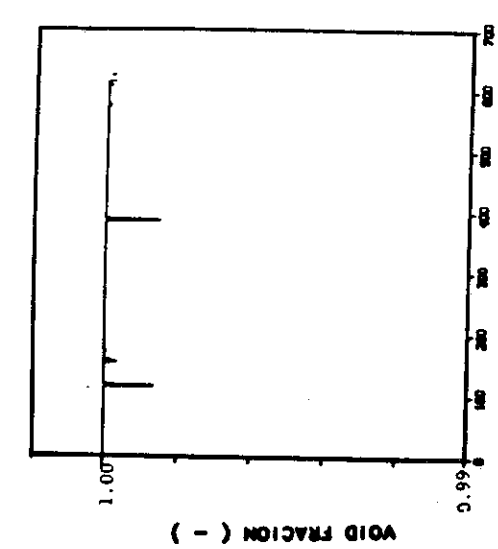

Fig. 18 Predicted void fraction in the intact hot leg.

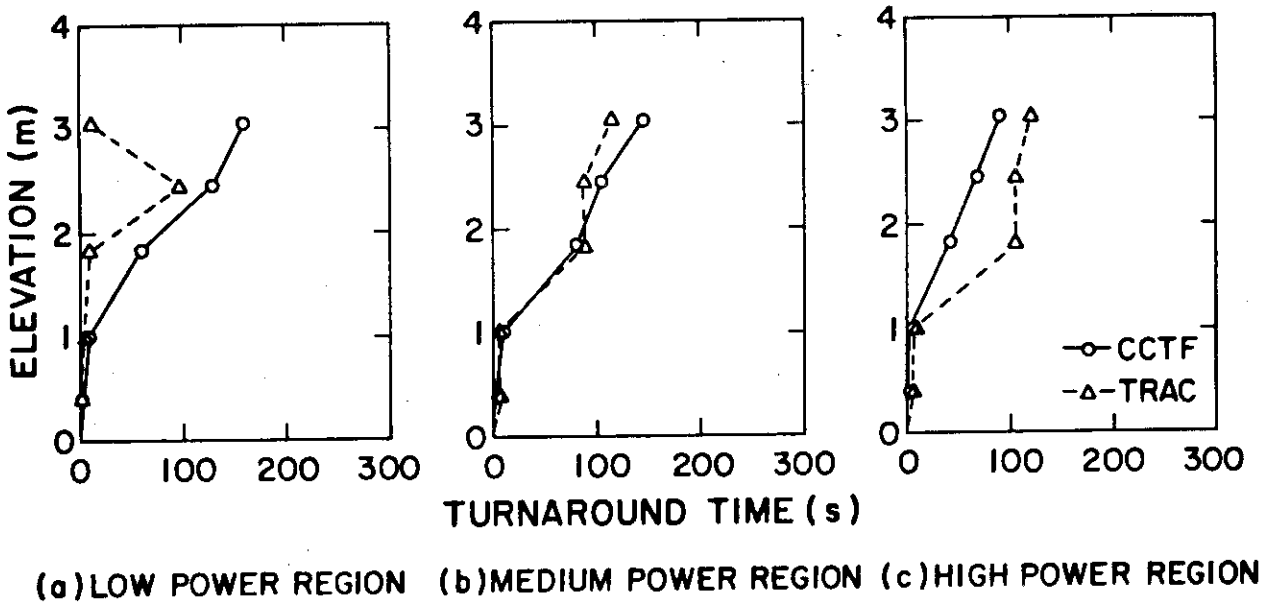

Fig. 20 Comparison of the turnaround time along the medium power rod in the high (radial peaking factor P_R = 1.299), medium (P_R = 1.092), and low (P_R = 0.841) power regions.

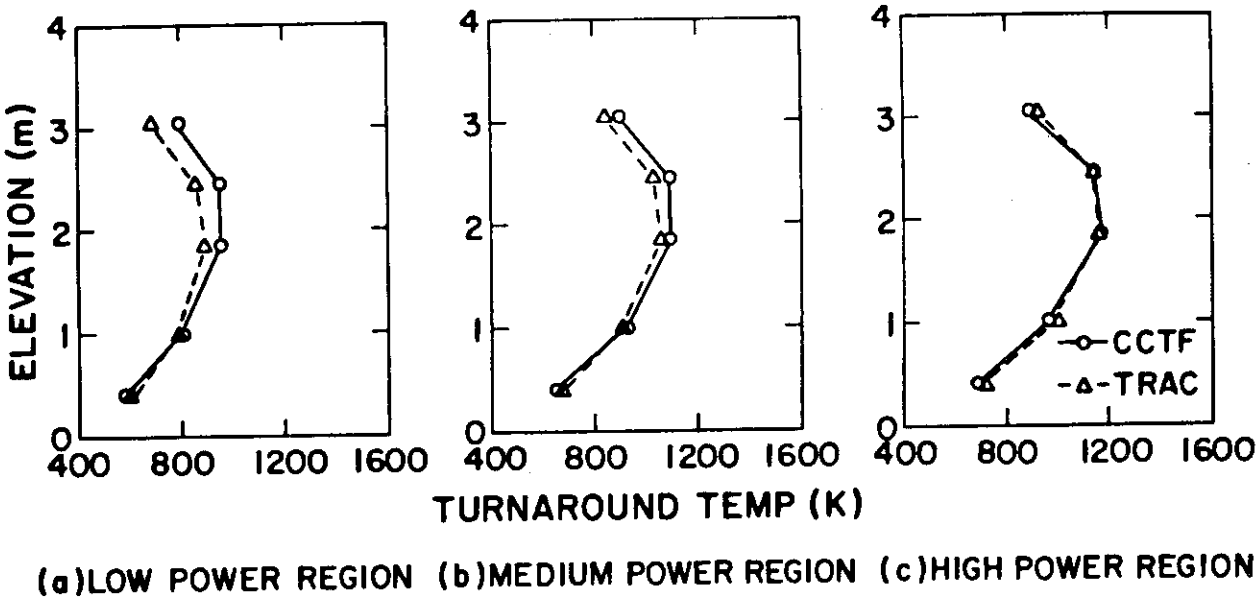

Fig. 21 Comparison of the turnaround temperature along the medium power rod in the high (radial peaking factor P_R = 1.299), medium (P_R = 1.092), and low (P_R = 0.841) power regions.

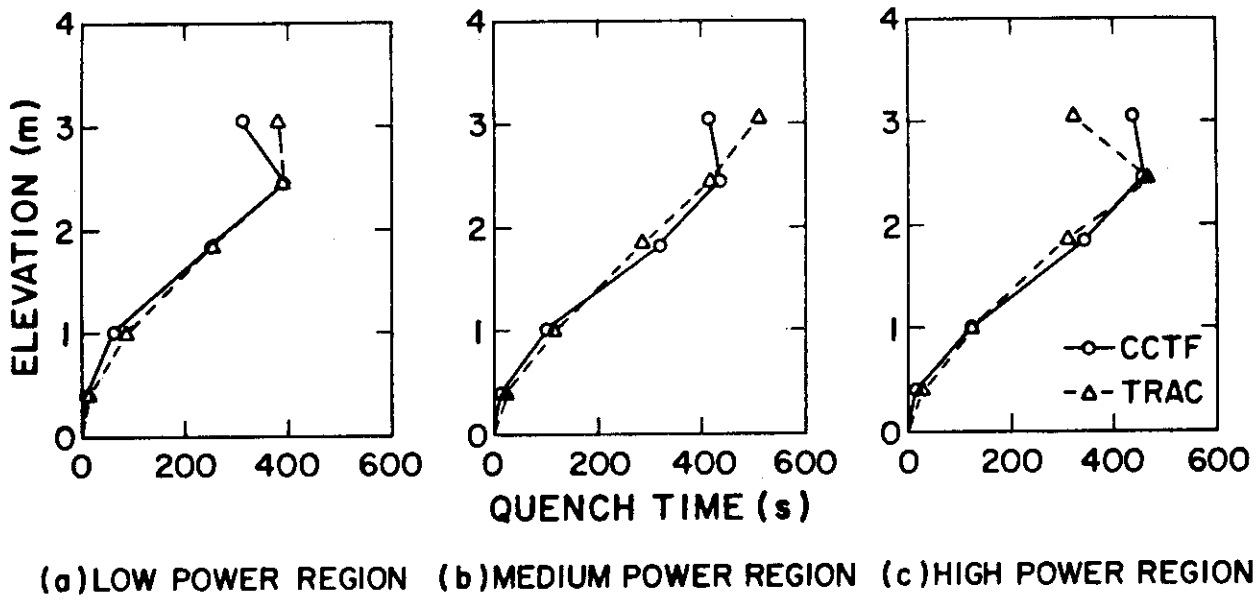

Fig. 22 Comparison of the quench time along the medium power rod in the high (radial peaking factor (P_R = 1.299), medium (P_R = 1.092), and low P_R = 0.841) power regions.

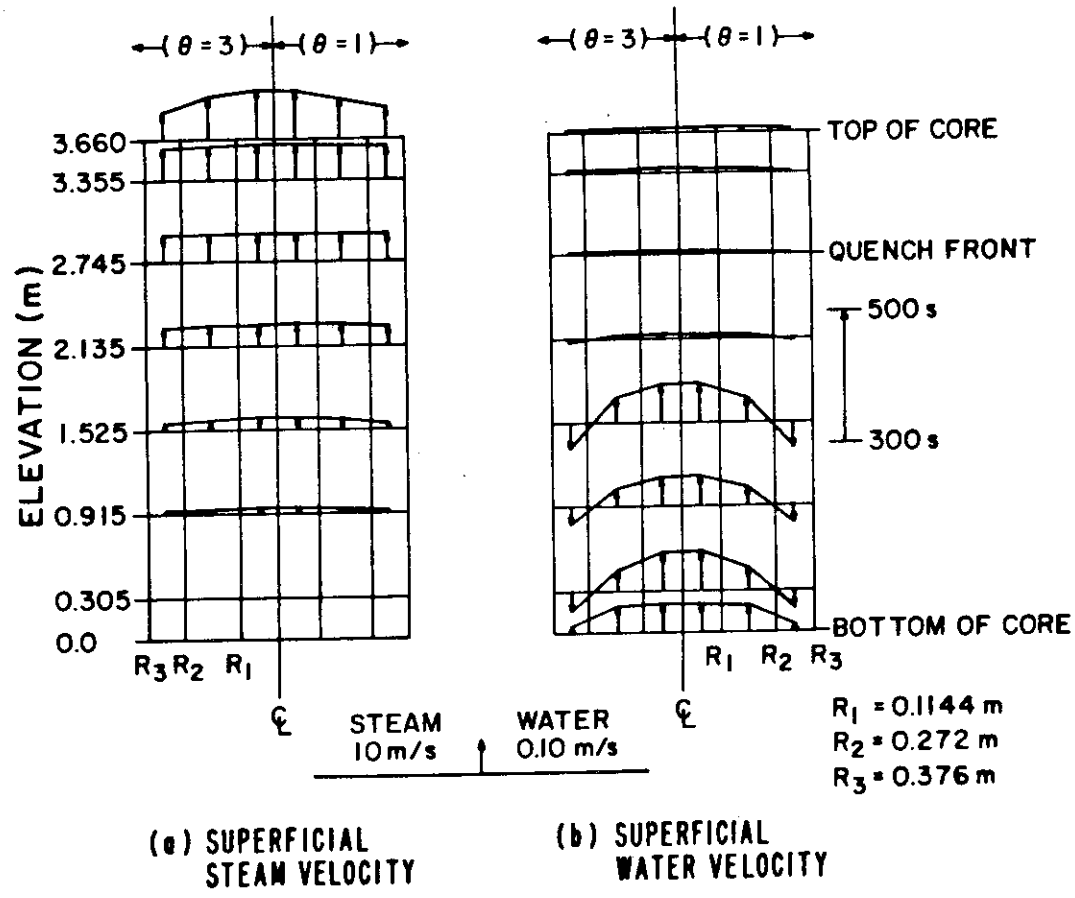

Fig. 23 Time-averaged superficial velocity(axial component) of steam and water in the core between 300 and 500 s.

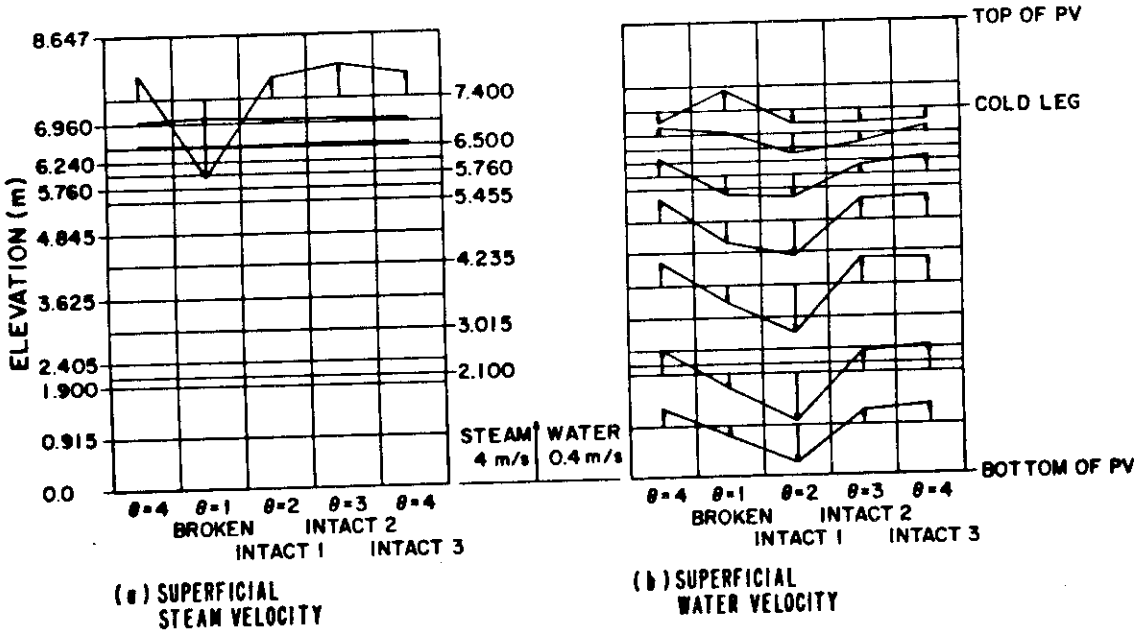

Fig. 24 Time-averaged superficial velocity (axial component) of steam and water in the downcomer between 300 and 500 s.

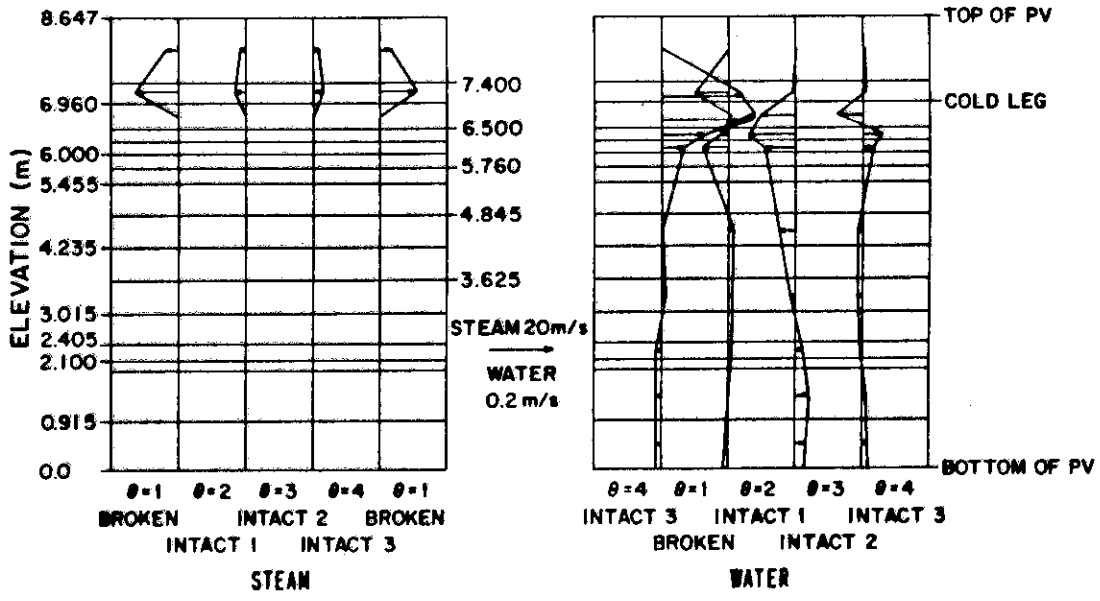

Fig. 25 Time-averaged azimuthal velocity of steam and water in the downcomer between 300 and 500 s.

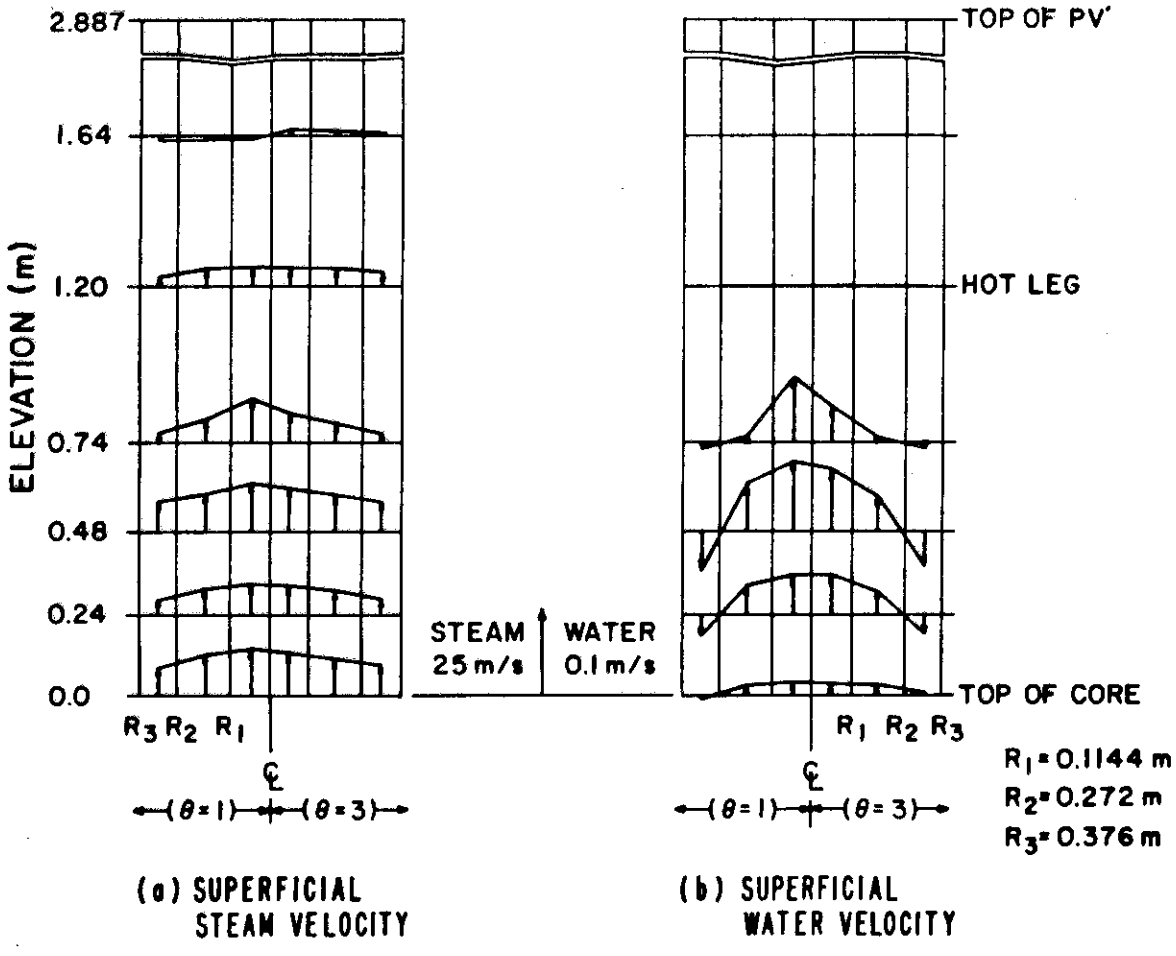

Fig. 26 Time-averaged superficial velocity (axial component) of steam and water in the upper plenum between 300 and 500 s.

APPENDIX A
MASS FLOW IN THE CORE

Figures A.1 through A.8 show the integral of the water, steam, and total mass flow rate in the Z direction of the core. The integration was performed with every 1/10 s data between 300 and 500 s. The Tag IDs have the general form of $IMXn_1Zn_2n_3$,

Where
- FT : total mass flow
- X = F : water mass flow
- FV : steam mass flow

n_1 : the level number in the TRAC model shown in Fig. 4,

n_2 : the radial ring number in the TRAC model shown in Fig. 4,

n_3 : the azimuthal sector number in the TRAC model shown in Fig. 4.

APPENDIX A
LIST OF FIGURES

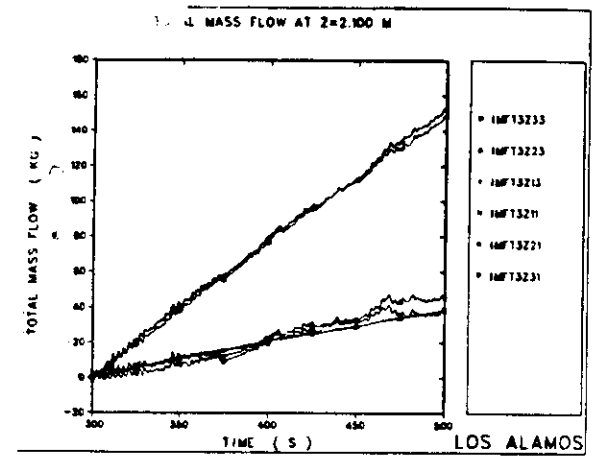

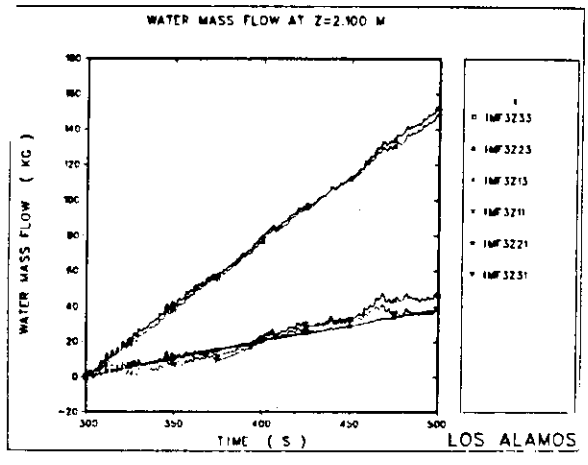

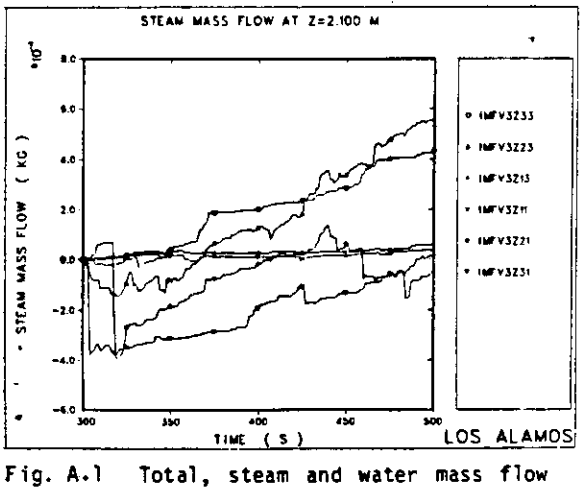

Fig. A.1 Total, steam and water mass flow at the elevation of 2.1 m (core inlet).

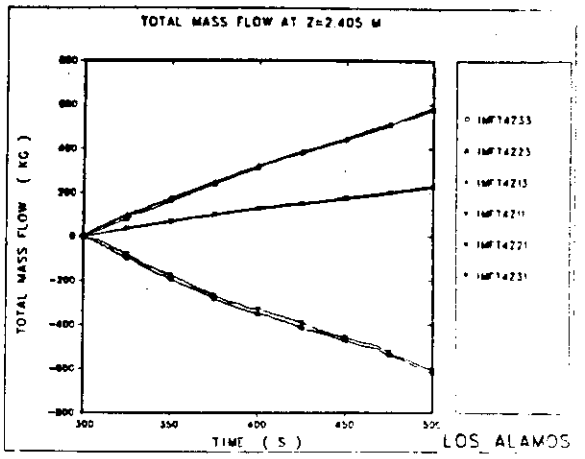

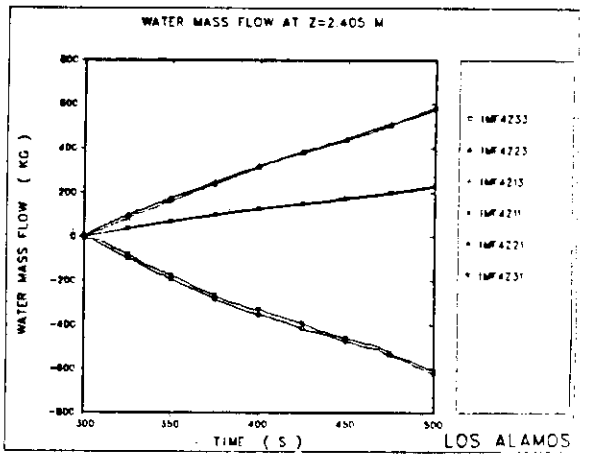

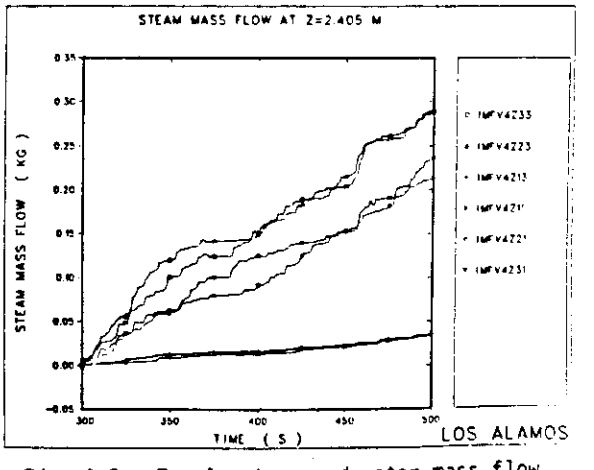

Fig. A.2 Total, steam and water mass flow at the elevation of 2.405 m.

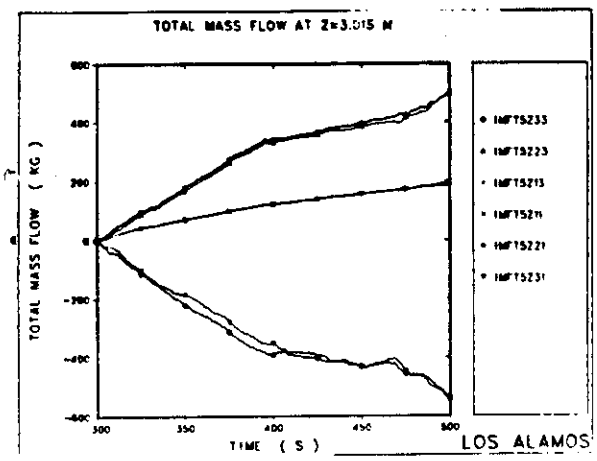

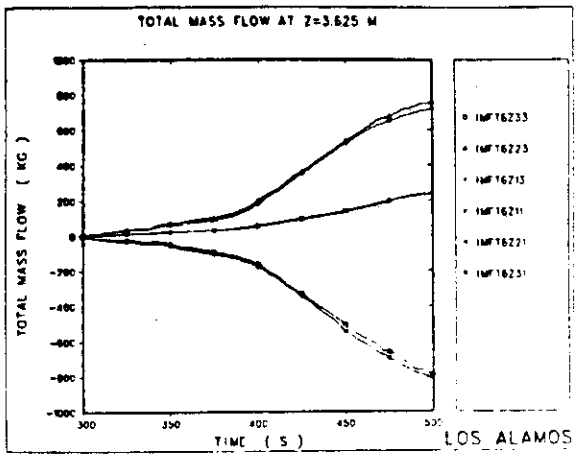

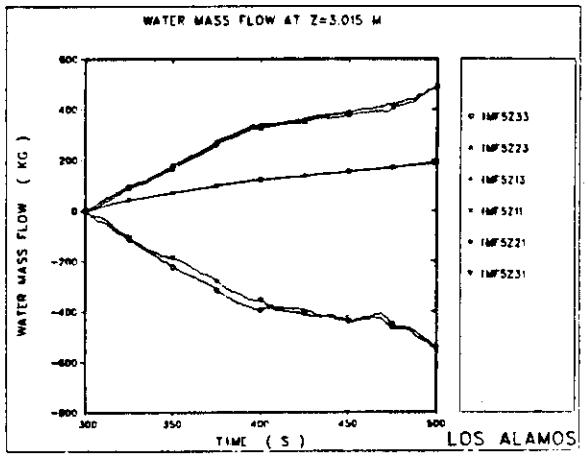

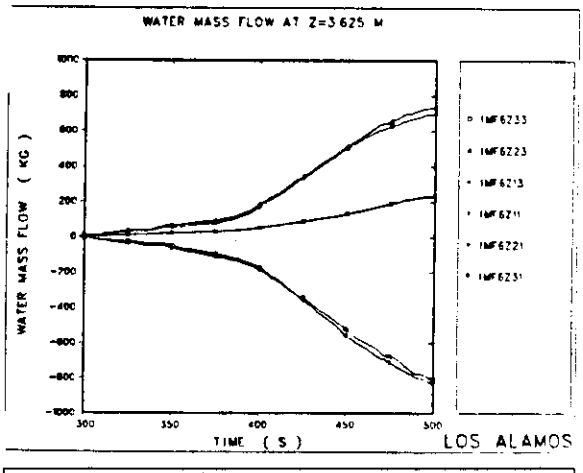

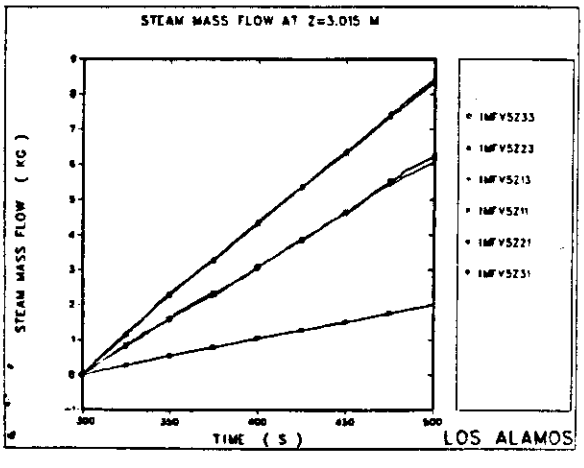

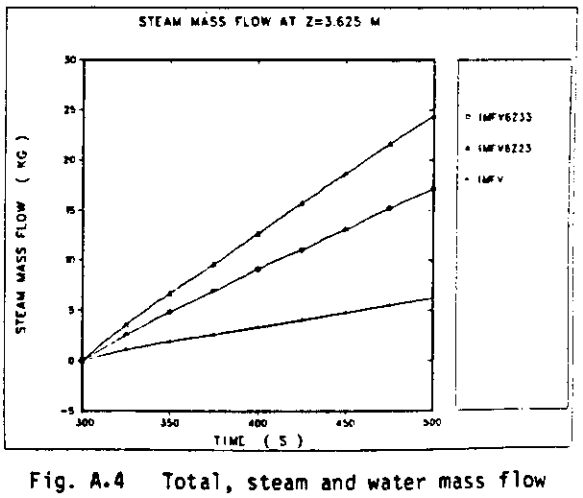

Fig. A.3 Total, steam and water mass flow at the elevation of 3.015 m.

Fig. A.4 Total, steam and water mass flow at the elevation of 3.625 m.

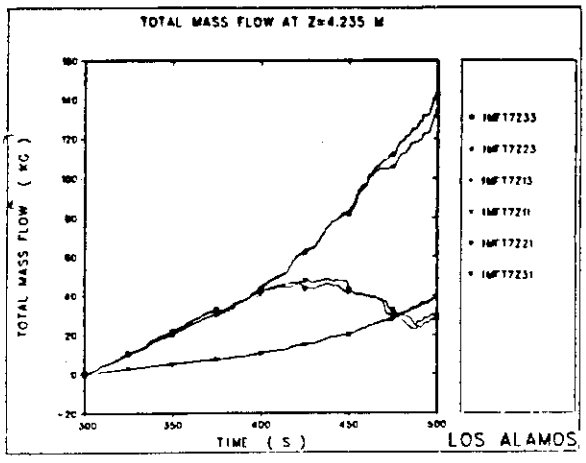

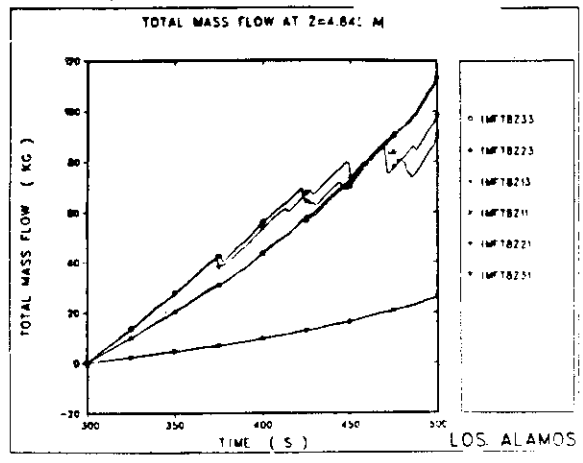

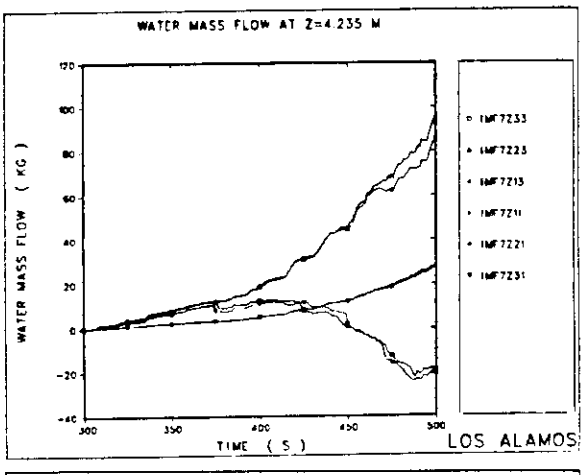

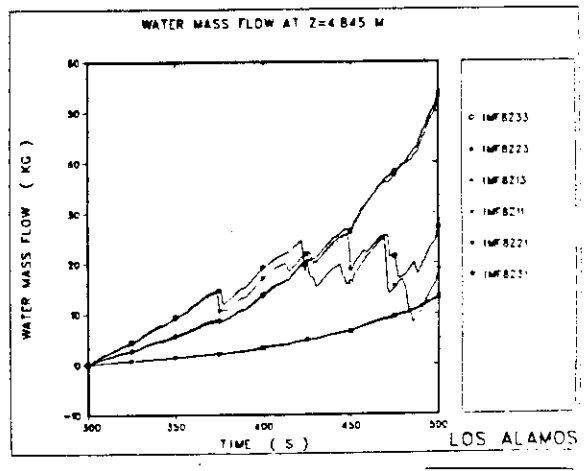

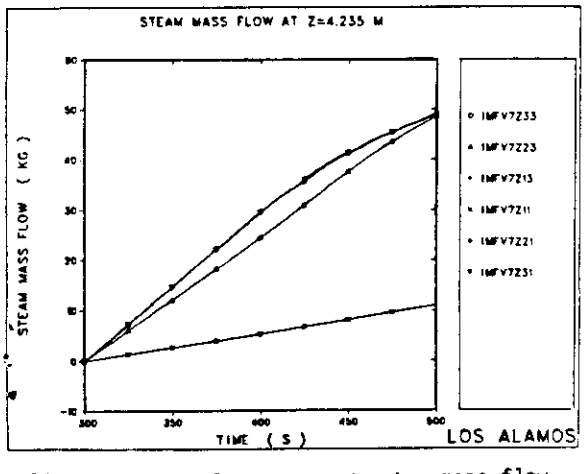

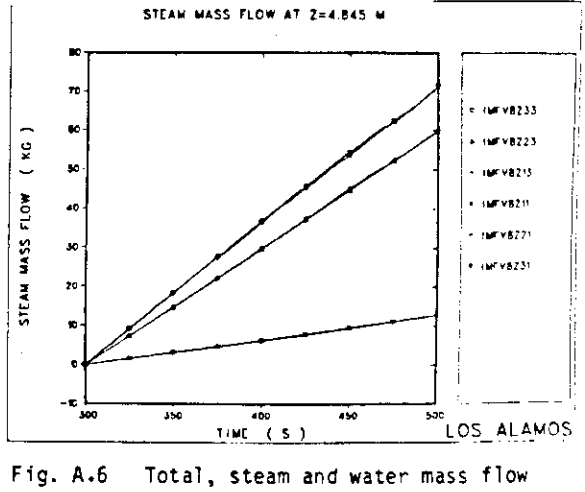

Fig. A.5 Total, steam and water mass flow at the elevation of 4.235 m.

Fig. A.6 Total, steam and water mass flow at the elevation of 4.845 m.

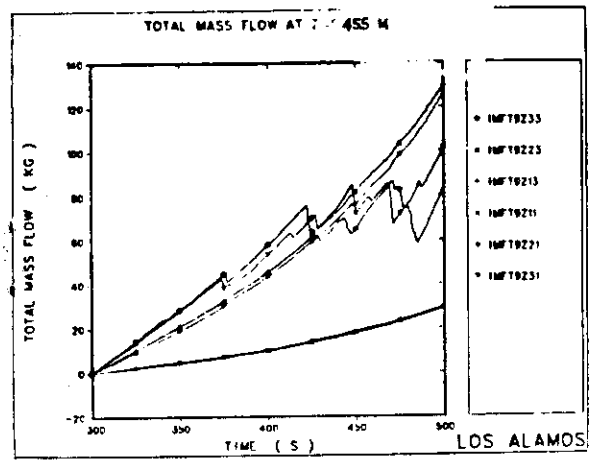

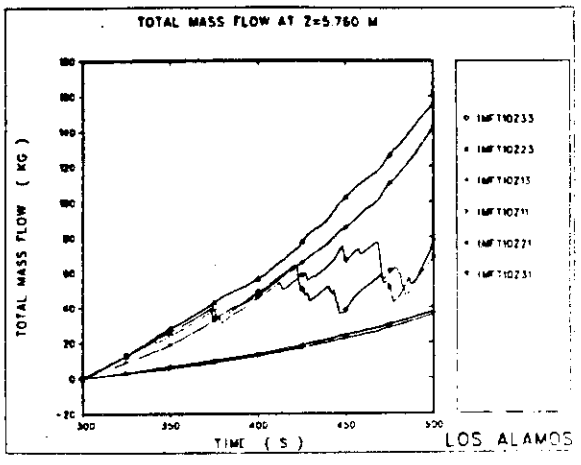

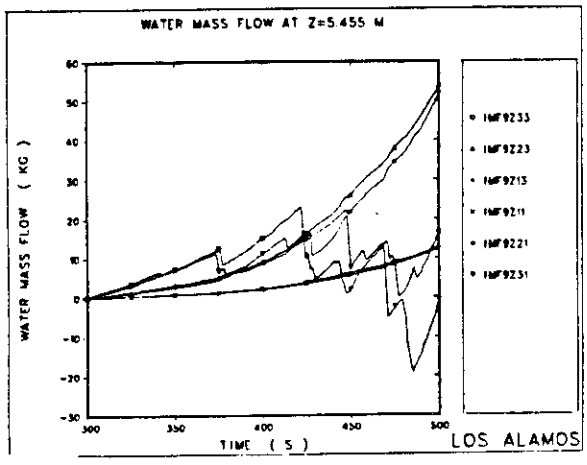

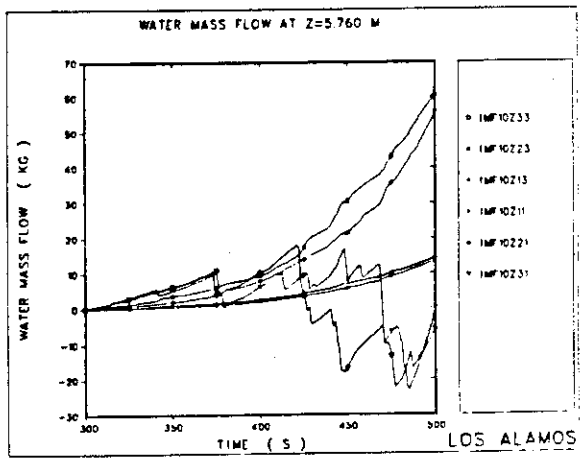

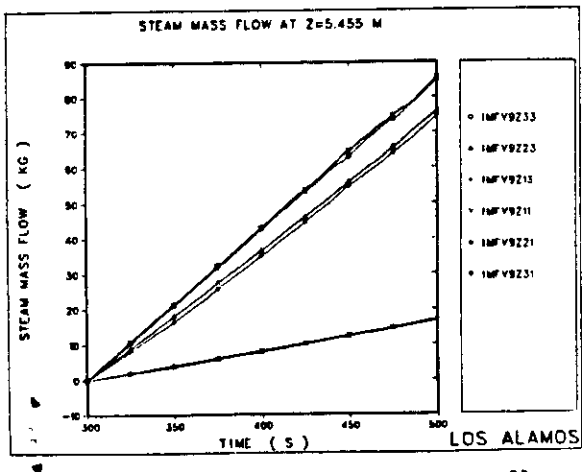

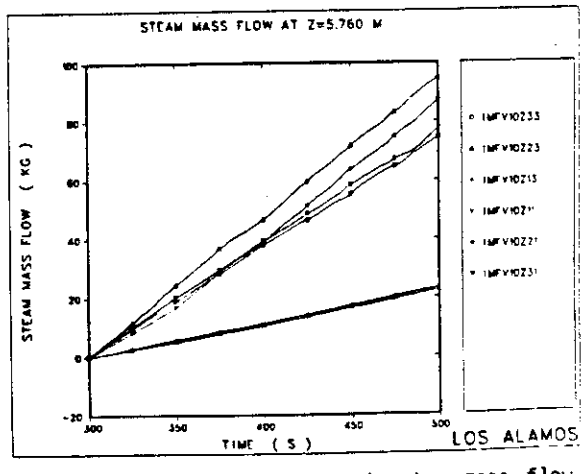

Fig. A.7 Total, steam and water mass flow at the elevation of 5.455 m.

Fig. A.8 Total, steam and water mass flow at the elevation of 5.76 m (core exit).